Green Chemistry

PAPER

View Article Online
View Journal | View Issue

Cite this: *Green Chem.*, 2016, **18**, 6046

Lignin depolymerization by fungal secretomes and a microbial sink†

Davinia Salvachúa,‡[a] Rui Katahira,‡[a] Nicholas S. Cleveland,[a] Payal Khanna,[a] Michael G. Resch,[a] Brenna A. Black,[a] Samuel O. Purvine,[b] Erika M. Zink,[b] Alicia Prieto,[c] María J. Martínez,[c] Angel T. Martínez,[c] Blake A. Simmons,[d,e] John M. Gladden[d,f] and Gregg T. Beckham*[a]

In Nature, powerful oxidative enzymes secreted by white rot fungi and some bacteria catalyze lignin depolymerization and some microbes are able to catabolize the resulting aromatic compounds as carbon and energy sources. Taken together, these two processes offer a potential route for microbial valorization of lignin. However, many challenges remain in realizing this concept, including that oxidative enzymes responsible for lignin depolymerization also catalyze polymerization of low molecular weight (LMW) lignin. Here, multiple basidiomycete secretomes were screened for ligninolytic enzyme activities in the presence of a residual lignin solid stream from a corn stover biorefinery, dubbed DMR-EH (Deacetylation, Mechanical Refining, and Enzymatic Hydrolysis) lignin. Two selected fungal secretomes, with high levels of laccases and peroxidases, were utilized for DMR-EH lignin depolymerization assays. The secretome from *Pleurotus eryngii*, which exhibited the highest laccase activity, reduced the lignin average molecular weight (M_w) by 63% and 75% at pH 7 compared to the M_w of the control treated at the same conditions and the initial DMR-EH lignin, respectively, and was applied in further depolymerization assays as a function of time. As repolymerization was observed after 3 days of incubation, an aromatic-catabolic microbe (*Pseudomonas putida* KT2440) was incubated with the fungal secretome and DMR-EH lignin. These experiments demonstrated that the presence of the bacterium enhances lignin depolymerization, likely due to bacterial catabolism of LMW lignin, which may partially prevent repolymerization. In addition, proteomics was also applied to the *P. eryngii* secretome to identify the enzymes present in the fungal cocktail utilized for the depolymerization assays, which highlighted a significant number of glucose/methanol/choline (GMC) oxidoreductases and laccases. Overall, this study demonstrates that ligninolytic enzymes can be used to partially depolymerize a solid, high lignin content biorefinery stream and that the presence of an aromatic-catabolic bacterium as a "microbial sink" improves the extent of enzymatic lignin depolymerization.

Received 4th June 2016,
Accepted 25th August 2016

DOI: 10.1039/c6gc01531j

www.rsc.org/greenchem

Introduction

Biological depolymerization of lignin has been studied extensively for the last several decades, built upon the discovery of several classes of powerful oxidative enzymes secreted by white rot fungi. These enzymes include laccases, oxidases such as aryl-alcohol oxidases (AAO) and glyoxal oxidases, and peroxidases such as manganese peroxidases (MnP), lignin peroxidases (LiP), versatile peroxidases (VP), and dye-decolorizing peroxidases (DyP).[1,2] Most of these enzymes exhibit wide substrate specificity and utilize radical intermediates for lignin depolymerization. More recently, the discovery of enzymes that are specific to particular linkages and stereochemistry has further broadened the scope of the enzymatic systems that

[a]*National Bioenergy Center, National Renewable Energy Laboratory (NREL), Golden, CO 80401, USA. E-mail: Gregg.Beckham@nrel.gov*
[b]*Environmental Molecular Sciences Laboratory, Pacific Northwest National Laboratory (PNNL), Richland, WA 99352, USA*
[c]*Centro de Investigaciones Biológicas, Consejo Superior de Investigaciones Científicas (CSIC), E-28040 Madrid, Spain*
[d]*Joint BioEnergy Institute (JBEI), Emeryville, CA 94608, USA*
[e]*Biological Systems and Engineering, Lawrence Berkeley National Laboratory, Berkeley, CA 94720, USA*
[f]*Sandia National Laboratory, Livermore, CA 94550, USA*
†Electronic supplementary information (ESI) available. See DOI: 10.1039/c6gc01531j
‡These authors contributed equally to this work.

microbes employ to depolymerize lignin.[3–5] Additionally, the realization that some bacteria can also secrete many of the same types of enzymes has indicated that biological lignin depolymerization is not limited to fungi.[6,7] Despite these efforts, the full extent of how ligninolytic enzymes work synergistically to depolymerize lignin, however, still remains somewhat unclear, which in turn limits our ability to rationally employ these powerful enzymes for industrial lignin depolymerization.[8] Several recent studies coupling proteomic analysis of fungal secretomes with detailed lignin characterization are providing deeper insights into how these interactions occur in Nature.[9,10]

Using enzymes to depolymerize lignin would ideally enable both the ability to remove lignin from biomass – a common objective in overcoming recalcitrance – and also produce aromatic compounds that could be isolated and converted to bioproducts – an emerging objective in biorefineries to improve overall process economics.[11] Despite significant promise, very few studies have effectively demonstrated robust lignin depolymerization using enzyme cocktails or isolated ligninolytic enzymes.[12–15] Challenges in this vein are many, including the fact that most oxidative enzymes used to depolymerize lignin are also capable of polymerizing aromatic compounds.[12,16] Moreover, obtaining lignin that maintains the natural linkages and molecular weight of the macromolecule in the plant cell wall is challenging, which can lead to results that do not reflect natural lignin breakdown processes. Indeed, many commercial lignins, such as Kraft lignin, are often heavily processed so that many natural linkages, including abundant ether bonds, have been cleaved and more refractory C–C bonds retained.[17,18] These factors, and others, have led to significant differences in the literature, making it challenging to compare between studies wherein enzymes are examined for lignin depolymerization.

Perhaps given the limited understanding of how ligninolytic enzymes function on natural substrates, most applications to date for these enzymes (*e.g.* laccases) are focused on their use as biocatalysts to bleach lignin-rich substrates for pulping processes,[19–22] as a pretreatment in bioethanol production,[13,23] as a proposed detoxification tool in ethanol fermentation *via* polymerization of phenolic compounds,[24] or in wastewater treatment.[25,26] However, in emerging biorefinery applications for lignin valorization, it would be ideal to depolymerize lignin to low molecular weight (LMW) compounds for the purpose of recovering and upgrading to bioproducts.[8,27,28] To effectively upgrade lignin to a single compound will require processes able to overcome the inherent heterogeneity of lignin. It has been recently proposed that aromatic catabolic microbes may be a potential solution for this problem *via* upper pathways that are able to convert heterogeneous slates of aromatic compounds into single intermediates, such as protocatechuate or catechol, and subsequently to central carbon metabolism.[8,27] A related hypothesis to how this concept occurs in Nature is that extracellular oxidative enzymes secreted by white rot fungi and bacteria produce a pool of available aromatic carbon, and, in response, microbes evolved pathways to utilize these compounds as carbon and energy sources.[7] These microbes thus operate as a "microbial sink" which could prevent extracellular repolymerization of LMW aromatic compounds (Fig. 1).

The aim of the current study is to examine how natural cocktails of ligninolytic enzymes depolymerize lignin in a solid, biorefinery substrate, and how the presence or absence of a microbe affects lignin depolymerization. The substrate of interest in this study originates from an emerging pretreatment that employs Deacetylation – mild alkaline treatment – followed by Mechanical Refining and Enzymatic Hydrolysis (DMR-EH).[29,30] This process generates high yields of hemicellulose and cellulose-derived sugars when used in combination with modern (hemi)cellulase cocktails, and is predicted to be cost competitive with standard deconstruction processes.[31] Given that this substrate has not experienced high temperatures or harsh chemical treatment that targets ether bonds, we hypothesized that the resulting lignin from this process will maintain many of the linkages present in native corn stover. In the current work, DMR-EH lignin is comprehensively characterized and used with 12 different fungal cultures to induce the production of ligninolytic enzymes. From these assays, a laccase-rich and a peroxidase-rich secretome were selected to examine *in vitro* depolymerization of DMR-EH lignin. For the laccase-rich cocktail from *Pleurotus eryngii*, which exhibited the highest extent of depolymerization, a proteomic analysis was also conducted to identify the enzymes responsible for the observed activity. Lastly, to test the hypothesis that the presence of a microbe can increase the extent of lignin depolymerization, the *P. eryngii* secretome and *Pseudomonas putida* KT2440 were combined, and the results indicate enhanced lignin depolymerization with the microbe present, demonstrating the concept of "microbial sink".

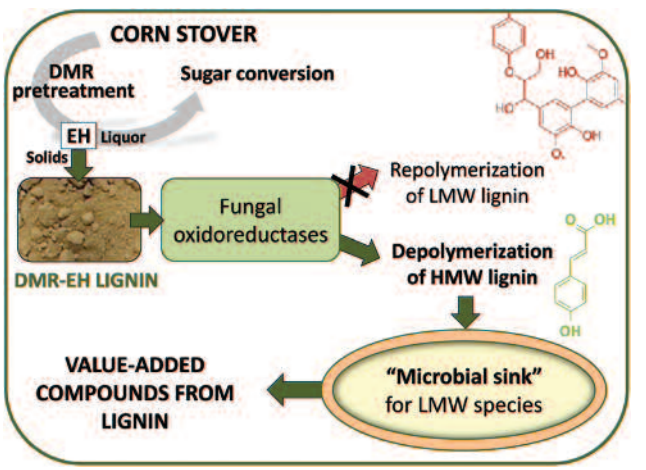

Fig. 1 Microbial sink concept. The presence of bacteria with ligninolytic enzymes, which are able to depolymerize high molecular weight (HMW) lignin, may act as a sink to avoid repolymerization of low molecular weight (LMW) aromatic compounds and enhance biological lignin depolymerization.

Results

Characterization of a biorefinery stream with native lignin-like properties

In the current study, the lignin-rich solid stream from the DMR-EH process was used as the solid substrate. DMR-EH lignin was characterized and compared to native corn stover *via* several methods. A full compositional analysis revealed that the lignin content in the residual DMR-EH solids is 60.0 wt% compared to the lignin in native corn stover at 14.8 wt% (Table 1). Residual polysaccharides from cellulose and hemicellulose were the second main component of this substrate, comprising 21.3 wt%, significantly lower than that in native corn stover (77%). These results demonstrate how DMR pretreatment generates a highly digestible substrate, enabling effective sugar recovery.

Table 1 Compositional analysis data of DMR-EH from corn stover. The amounts are shown as wt% on a dry weight basis

	Corn stover (%)	DMR-EH
Lignin	**14.80**	**60.00**
Ash	2.54	2.18
Glucan	36.48	9.24
Xylan	30.18	9.36
Galactan	1.76	1.04
Arabinan	3.52	1.62
Acetate	2.71	0.72
Proteins	NA	6.07
Total mass balance	**91.99**	**90.23**

NA: not analyzed.

Gel permeation chromatography (GPC) was conducted to measure the molecular weight distribution, shown in Fig. 2A. It is noteworthy that considering both sample preparation and GPC method, which employs a diode array detector with absorbance at 260 ± 40 nm, only lignin should be observed in this analysis (see Materials and methods). The GPC profile reveals that DMR-EH exhibits a large amount of high molecular weight (HMW) lignin (>~1300 Da), with an average molecular weight (M_w) of 9200 Da. When analyzing GPC data, three additional parameters are also reported: the number average molecular weight (M_n), peak molecular weight (M_p) and polydispersity (PD). The M_n of DMR-EH lignin is 2100 Da. The M_p is 3900 Da, indicating that the most abundant molecule is 3900 Da, and the PD value reflects the distribution of molecular weight. High values for PD (*e.g.*, >3), as the observed in the current substrate (PD 4.4), indicates that the molecular weight distribution of DMR-EH lignin is broad. These four parameters M_w, M_n, M_p, and PD will be presented in this study.

A 2D-nuclear magnetic resonance (NMR) spectrum of DMR-EH was also collected to obtain chemical information

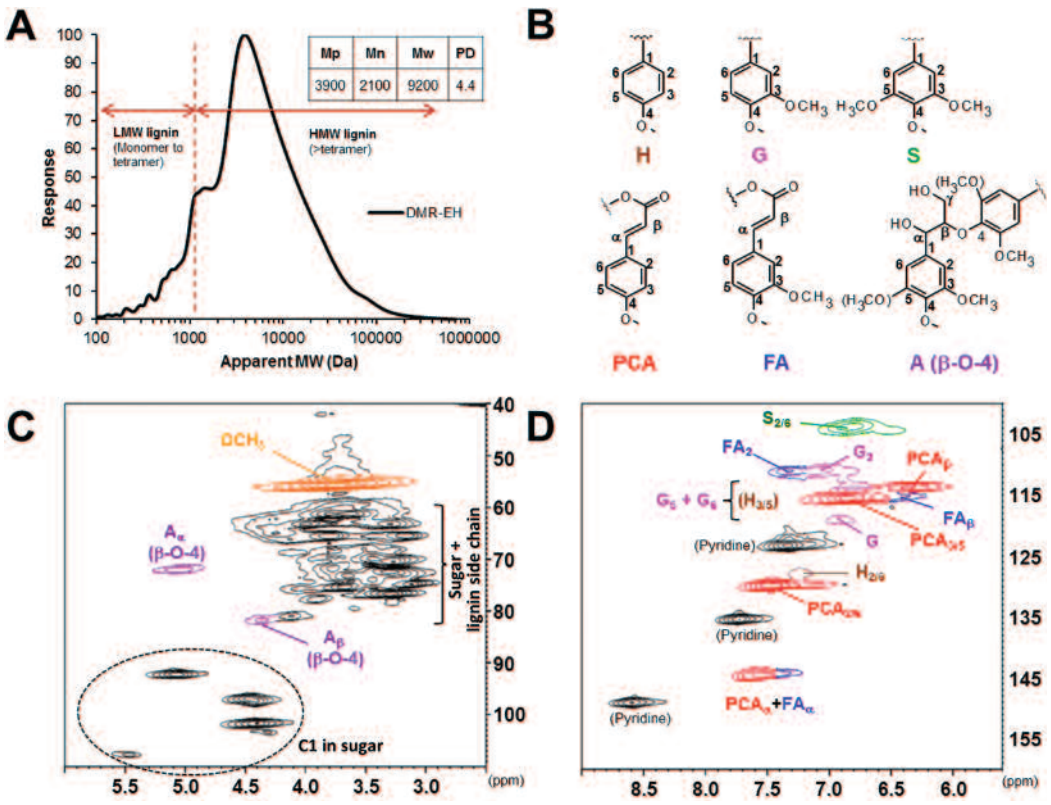

Fig. 2 Characterization of DMR-EH lignin. (A) GPC chromatogram of DMR-EH. LMW = low molecular weight; HMW = high molecular weight. M_p, M_n, M_w, and PD values correspond to DMR-EH lignin. (B) Structures identified in lignin. H: *p*-hydroxyphenyl units, G: guaiacyl units; S: syringyl units; A: β-O-4 alkyl aryl ethers; PCA: *p*-coumaric acid; FA: ferulic acid. (C) Expanded HSQC NMR spectrum of DMR-EH lignin side chain region (δ_C/δ_H 40–110/2.5–6.0 ppm). (D) Expanded HSQC spectrum in aromatic region (δ_C/δ_H 100–160/5.5–9.0 ppm). Solvent: d_6-DMSO : d_5-pyridine (4 : 1, v/v).

related to the lignin composition and interunit linkages and remaining carbohydrates. The Heteronuclear Single Quantum Coherence (HSQC) NMR spectrum consists of three regions: the saturated non-oxygenated aliphatic region (δ_C/δ_H 10–40/0.5–3.0 ppm), the lignin side chain and carbohydrate region (δ_C/δ_H 50–110/2.8–5.7 ppm), and the aromatic region (δ_C/δ_H 100–165/6.3–8.0 ppm). The expanded spectra for the side chain and aromatic regions are shown in Fig. 2C and D, respectively. The typical lignin units and linkages in herbaceous biomass are shown in Fig. 2B (H: *p*-hydroxyphenyl units, G: guaiacyl units; S: syringyl units, A: β-O-4 alkyl aryl ethers; PCA: *p*-coumaric acid; FA: ferulic acid). Signals were assigned from previously reported HSQC data.[32–35] In the HSQC spectrum in the side chain region (Fig. 2C), signals at δ_C/δ_H 70–73/4.8–5.3 and 81–83/4.3–4.5 ppm are assigned to the Cα/Hα and Cβ/Hβ positions in β-O-4 structures. A methoxyl peak appears at δ_C/δ_H 54–57/3.1–4.5 ppm. Anomeric carbon peaks in the carbohydrates are present at δ_C/δ_H 92–110/4.1–5.6 ppm. Broad peaks in the region of δ_C/δ_H 58–80/2.9–4.6 ppm are also from carbohydrates. Few correlation peaks of other interunit linkages (resinol, phenylcoumaran, spirodienone) were detected, meaning that the DMR-EH lignin exhibits mainly β-O-4 structures. In the HSQC spectrum of the DMR-EH lignin aromatic region (Fig. 2D), peaks of H, G, S, PCA, and FA units were observed. Peaks in main units of H, G, and S appeared as follows: the ^{13}C–^{1}H correlation for S2/6 was at δ_C/δ_H 104.1/6.7, G2 at δ_C/δ_H 110.6/7.0, and G5/6 at 113–120/6.6–7.1 ppm, respectively. The correlations of C2/6 and Cβ in PCA units were found at δ_C/δ_H 130/7.48 and 114.0/6.4 ppm, respectively. The resonance from Cβ in FA is minimal at δ_C/δ_H 115/6.38 ppm. The signals from the Cα positions in PCA and FA overlapped at δ_C/δ_H 144.7/7.6–7.4.

Screening of oxidoreductase activity in the secretome of 12 white-rot fungi

Oxidoreductases are the main oxidative enzymes involved in lignin depolymerization by fungi.[1] As such, the activities of diverse oxidoreductases were evaluated in the secretomes of twelve white-rot fungi grown in submerged cultures in the presence of DMR-EH lignin. The fungi selected for this study were *Bjerkandera* sp., *Bjerkandera adusta*, *Cerioporopsis subvermispora*, *Irpex lacteus*, *Panus tigrinus*, *Phanerochaete chrysosporium*, *Phellinus robustus*, *Pleurotus eryngii*, *Pleurotus ostreatus*, *Polyporus alveolaris*, *Stereum hirsutum*, and *Trametes versicolor*. Spectrophotometric (visible and UV) assays were used to evaluate the activity of the following enzymes: laccases, AAO, and various peroxidases such as LiP, MnP, VP, and DyP. Overall, the fungi exhibit substantial differences in both enzyme diversity and time-dependent activity profiles in the assay conditions. Fig. 3 shows the results from the six species that displayed the highest laccase and/or peroxidase activities from the twelve fungi (Fig. S1†). *P. eryngii*, for instance, produced the highest levels of laccase, up to 7 U mL^{-1}, between 7 and 9 days of incubation (Fig. 3D). AAO was also detected in the same secretome, peaking at 7 days and reaching 145 mU mL^{-1}. Conversely, *Bjerkandera* sp., mainly produced peroxidases

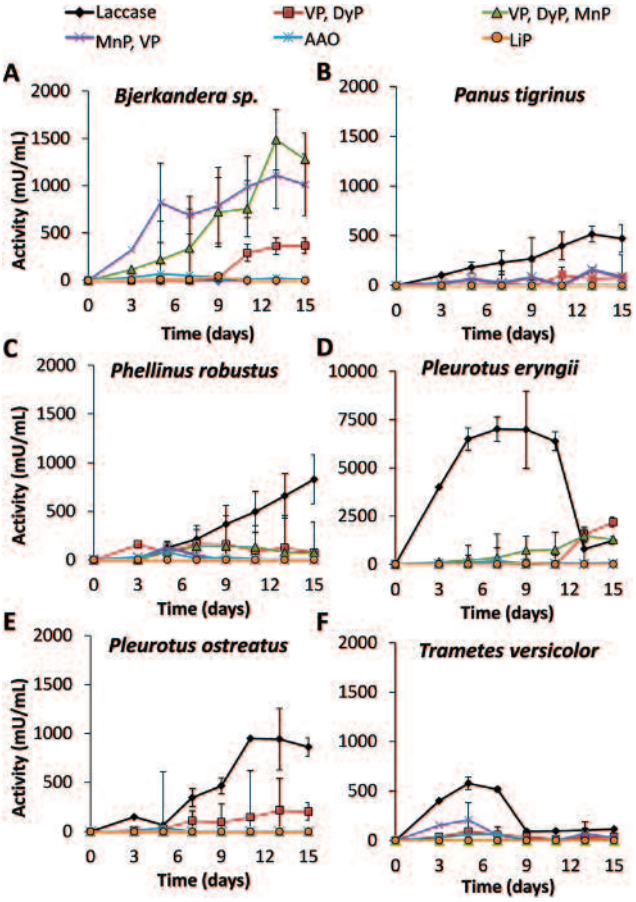

Fig. 3 Detection of oxidoreductases in the secretome of six white-rot fungi. Enzymes activities are presented for the fungi (A) *Bjerkandera* sp., (B) *P. tigrinus*, (C) *P. robustus*, (D) *P. eryngii*, (E) *P. ostreatus*, and (F) *T. versicolor*. Oxidoreductase activity was followed by the oxidation of different substrates (see Materials and methods). It is noteworthy that the oxidation of the same substrate can be the result of the action of different enzymes. In brief, the substrates and pH utilized for the enzyme screening were: 2,2′-azino-bis(3-ethylbenzthiazoline-6-sulfonic acid) (ABTS) at pH 5 for laccases; veratryl alcohol at pH 5 for AAO; $MnSO_4$ with H_2O_2 for MnP and VP; veratryl alcohol with H_2O_2 at pH 3 for LiP; ABTS with H_2O_2 at pH 5 for both VP and DyP; and ABTS with $MnSO_4$ and H_2O_2 at pH 5 for VP, DyP, and short-MnP.[38] Laccase activity was subtracted from peroxidase activity when both enzymes were present and ABTS was used as substrate.

throughout the incubation, reaching values up to 1.5 U mL^{-1} (Fig. 3A). To ascertain the type of peroxidases secreted by this fungus, enzyme assays using different dyes were employed. Discoloration was positive for an azo-dye, but not an anthraquinone dye, suggesting that it is not a DyP-type peroxidase but most likely a VP, although anthraquinone discoloration has been also recently reported for this type of enzyme.[36] AAO was also detected in the *Bjerkandera* sp. secretome, peaking at 5 days at 65 mU mL^{-1}. *P. tigrinus* (Fig. 3B), *P. robustus* (Fig. 3C), *P. ostreatus*, and *T. versicolor* (Fig. 3E) produced both laccases and peroxidases throughout the incubation, but at levels lower than reported above. As such, *P. eryngii* and *Bjerkandera* sp. were selected to produce larger

volumes of secretome to perform depolymerization assays on DMR-EH lignin.

Depolymerization of DMR-EH lignin with fungal secretomes containing high laccase and peroxidase activity

Lignin depolymerization assays were performed at pH 4.5 and 7. The former pH was selected because it is close to the optimal for standard ligninolytic enzyme function[37] and the latter because lignin is well known to be more soluble at higher pH. Moreover, pH 7 was also chosen as it is close to the optimal for typical bacterial growth, in preparation for the microbial sink experiments reported below. Laccases from *P. eryngii* exhibit approximately 3-fold lower activity at pH 7 than 4.5. Peroxidase activity from the *Bjerkandera* sp. secretome was only detected at pH 4.5, and as such depolymerization assays were only performed at pH 4.5 (with H_2O_2 and Mn^{2+}) for this cocktail. Different enzymes dosages were also tested, expressed as U of enzyme (at the corresponding pH and using ABTS as substrate) per g of DMR-EH.

GPC was utilized to analyze lignin depolymerization in the insoluble fraction of DMR-EH after 3 and 6 days of enzyme treatment (Fig. 4, Table S1†). The control samples (non-enzymatically treated and incubated during 6 days in the same conditions than the enzyme treated samples) exhibit different molecular weights depending on the pH; namely the lignin M_w is approximately 50% higher at pH 4.5 (12 000 Da) (Fig. 4A) than at pH 7 (6100 Da) (Fig. 4B). GPC parameters from both controls at pH 4.5 in the presence (Fig. 4C and D) and the absence of H_2O_2 and Mn^{2+} (Fig. 4A) were similar.

For the enzyme-treated samples, generally, higher enzyme dosages produced greater decreases of lignin M_w. The lone exception to this is the treatment from the *Bjerkandera* sp. secretome, which increased M_w at the lowest enzyme dosage compared to the control. Peroxidases from *Bjerkandera* sp. (80 U g^{-1}) decreased lignin M_w by 54% at 6 days, while *P. eryngii* laccases (100 U g^{-1}) decreased lignin M_w by 55% and 63% at pH 4.5 and 7, respectively, after 3 days of incubation. However, laccases and peroxidases combined at pH 4.5 at the highest dosages decreased M_w by 84%, reaching the lowest lignin M_w in the current study (2000 Da) (Fig. 4D). The most dramatic changes, in terms of release of LMW lignin species, were observed in treatments with the *P. eryngii* secretome at pH 7 and 30 U g^{-1} at both 3 and 6 days but also when utilizing mixed secretomes at pH 4.5. It is also notable that treatments at 3 days produced lower lignin M_w than at 6 days when the *P. eryngii* secretome was present – most likely due to repolymerization. Based on the results in Fig. 4, we selected the treatments at pH 7 with the *P. eryngii* secretome for further examination of lignin depolymerization since (1) these treatments produce the second lowest lignin M_w, releasing considerable LMW lignin compounds, (2) laccases do not require addition of co-factors such as H_2O_2 and Mn^{2+}, and (3) pH ~7

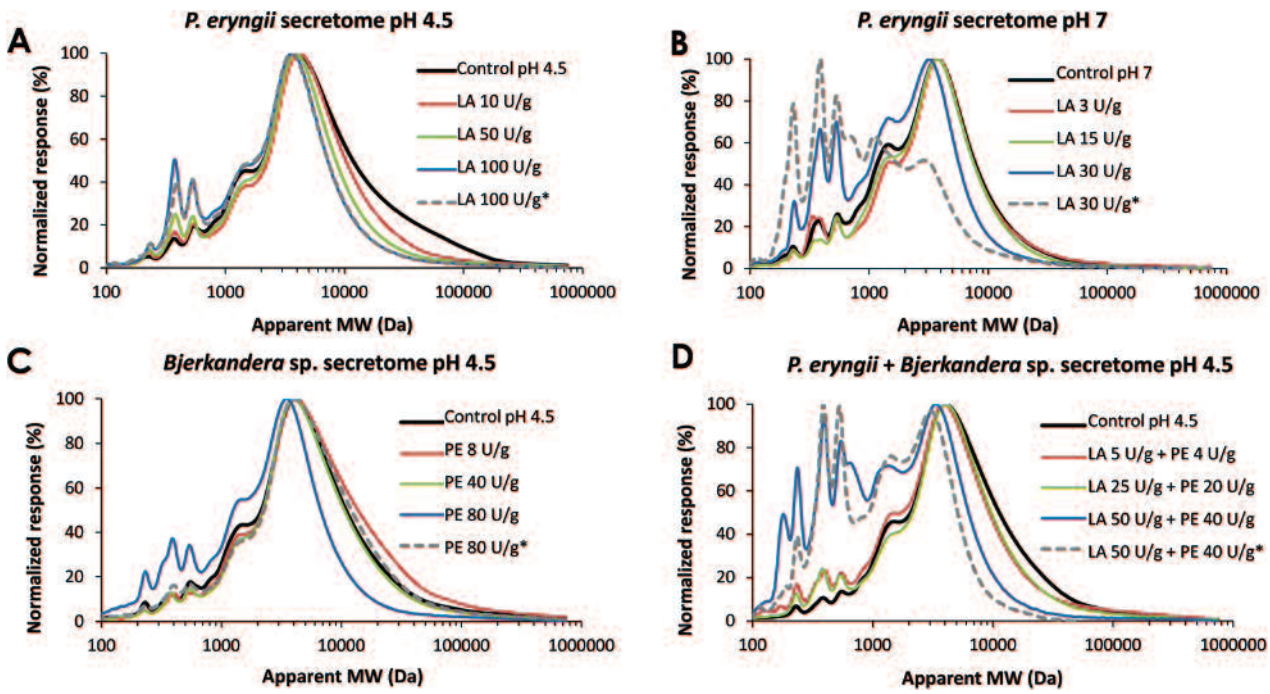

Fig. 4 GPC results from DMR-EH lignin before and after the enzyme treatments with the fungal secretomes at 3 and 6 days. Graphs show the results from treatments with the *P. eryngii* secretome at (A) pH 4.5 and (B) pH 7, treatments with (C) *Bjerkandera* sp. secretome at pH 4.5, and treatments with (D) both fungal secretomes at pH 4.5. Enzyme treatments on DMR-EH lignin were conducted over 3 (dashed lines) and 6 (solid lines) days at 30 °C and 150 rpm. H_2O_2 and Mn^{2+} were added periodically to treatments containing peroxidases and to the corresponding controls (CTL). Enzyme dosages are expressed as U of enzyme per gram of DMR-EH lignin. Laccase (LA) and peroxidase (PE) activities were calculated following the oxidation of ABTS at the corresponding pH in the absence or the presence of Mn^{2+} and H_2O_2, respectively. The asterisk (*) highlights 3-day treatments.

was required for further complementary bacterial assays. Moreover, due to results found at 3 days of treatment compared to 6 days, the incubation time was shortened.

DMR-EH lignin depolymerization at pH 7 as a function of time with the *P. eryngii* secretome

Subsequently, an experiment was performed over 4 days with the *P. eryngii* secretome to understand how depolymerization occurs as a function of time at pH 7. DMR-EH lignin was treated with similar laccase dosages from the previous section (3, 10, and 30 U g^{-1}) and the insoluble fraction analyzed by GPC every 24 h. Different to the previous experiment, DMR-EH lignin was autoclaved before the enzyme treatments since, for further experiments in the presence of bacteria, substrate sterilization is required; this is the main difference between the experiments shown in Fig. 4 and 5 and is likely responsible for the differences in molecular weight changes. In addition, for comparison purposes, a parallel experiment was conducted with a dialyzed secretome to remove possible aromatics, growth media, or fungal metabolites remaining in the secretome that could interfere in the depolymerization assays or later in the bacterial treatments.

Fig. 5(A–C) and Table S2† shows the GPC profiles and other GPC parameters from this experiment. There are not substantial differences among the treatments using non-dialyzed and dialyzed secretomes (Fig. 5B and C). In all three cases, the depolymerization trends exhibit an early release of LMW lignin species and a corresponding reduction of HMW lignin until the third day of treatment, followed by an increase in HMW lignin at 4 days. These trends were observed in all the treatments, but are more evident when using the highest laccase dosage (Fig. 5D), especially in the release of LMW lignin species (<1000 Da). Fig. 5D illustrates the M_w of DMR-EH lignin and presents all the parameters obtained from GPC in those treatments with the non-dialyzed secretome. Higher enzyme dosages resulted in a higher extent of depolymerization. The lignin M_w decreased compared to the control (at 4 days and with inactivated secretome) by 25, 37, and 45% when using 3, 10, and 30 U of laccase per g of substrate at 3 days, respectively. It is noteworthy that the control using boiled (inactivated) secretome gave similar profiles (data not shown) and numbers (Fig. 5D) than the control with buffer alone, suggesting that there are not critical interactions between the substrate and the enzymes that could interfere during the processing and analysis of the samples, and thus the results.

To further understand depolymerization and repolymerization, changes in the DMR-EH lignin structure after the enzyme treatment were evaluated by 2D-NMR. Fig. 6 and 7 show the HSQC NMR spectra of the DMR-EH, DMR-EH control (after autoclaving), and the treated DMR-EH at 2, 3 and 4 days. Expanded HSQC spectra in the lignin side chain and carbohydrate region are shown in Fig. 6. The correlation peaks of Cα and Cβ in the β-O-4 structure appear at δ_C/δ_H 71/5.05 and 82/4.3 ppm, respectively. Both peaks decreased in 2 and 3 days, but the Cα peak intensity did not change in 4 days. This implies that β-O-4 structures were broken gradually by laccases releasing phenolic compounds, and then cleavage of

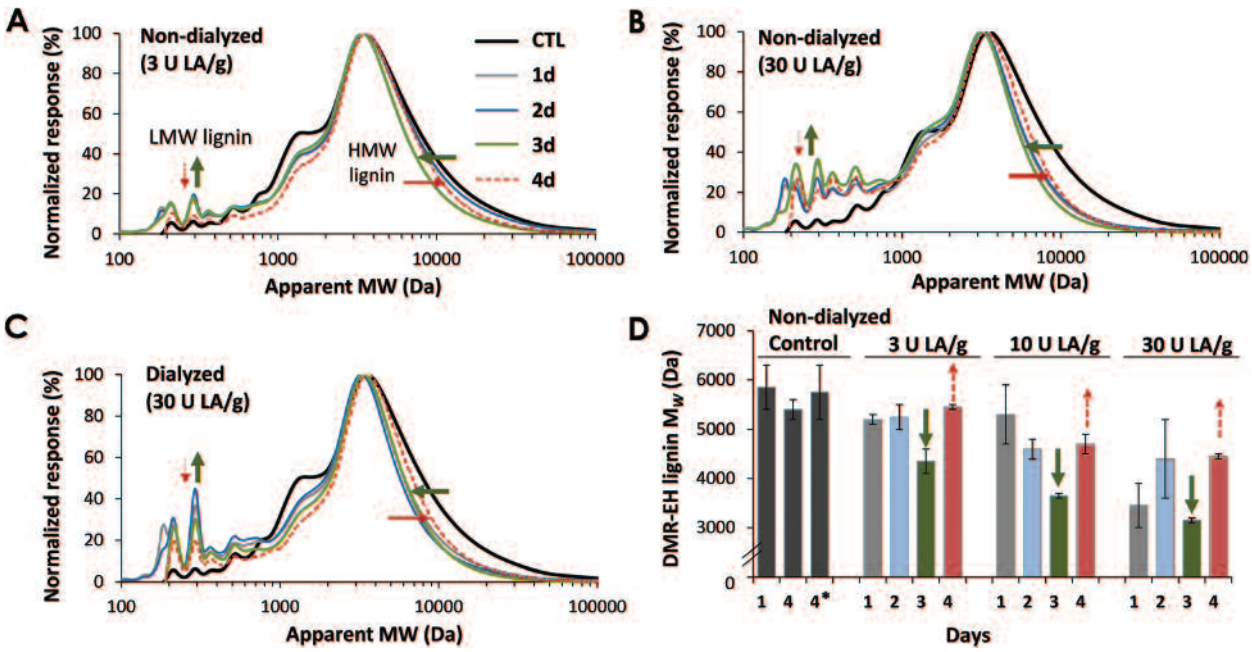

Fig. 5 GPC profiles of DMR-EH lignin as a function of time from *P. eryngii* secretome treatments at pH 7 over 4 days of incubation. Graphs show the DMR-EH lignin M_w profile from treatments with (A) 3 U laccase (LA) per g from non-dialyzed secretome, (B) 30 U LA per g from non-dialyzed secretome, (C) 30 U LA per g from dialyzed secretome, and (D) DMR-EH lignin M_w by using different laccase dosages from non-dialyzed secretomes. Green continuous arrows highlight the highest depolymerization extent at 3 days of treatment. Red discontinuous arrows indicate the increase in lignin M_w possibly *via* repolymerization. The asterisk (*) at 4 days corresponds to the control that contains boiled secretome.

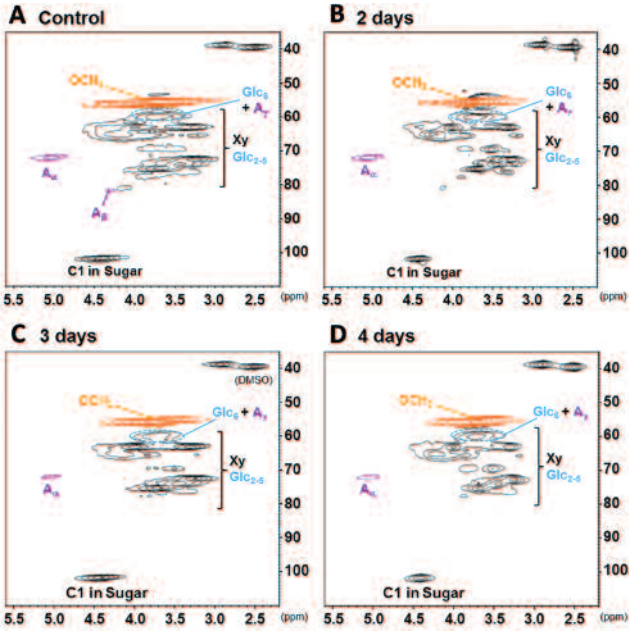

Fig. 6 Expanded HSQC NMR spectra in lignin side chain and carbohydrate region (δ_C/δ_H 35–110/2.2–5.6 ppm) of solid residues before and after enzyme treatments for 2–4 days with non-dialyzed secretome. (A) DMR-EH control (autoclaved) without enzyme, (B, C, D) 2, 3, and 4 days of treatment with *P. eryngii* secretome containing 30 U laccase per g. The Cβ peak at δ_C/δ_H 82/4.3 ppm decreased, but does not disappear after 2, 3 and 4 days. The peak shows if the lower contour level in HSQC spectrum is selected. However, under the lower contour level, the noisy peaks also show and methoxyl peak overlaps with the sugar peaks. In order to keep important peaks clear, the HSQC NMR spectra with a high contour level was selected.

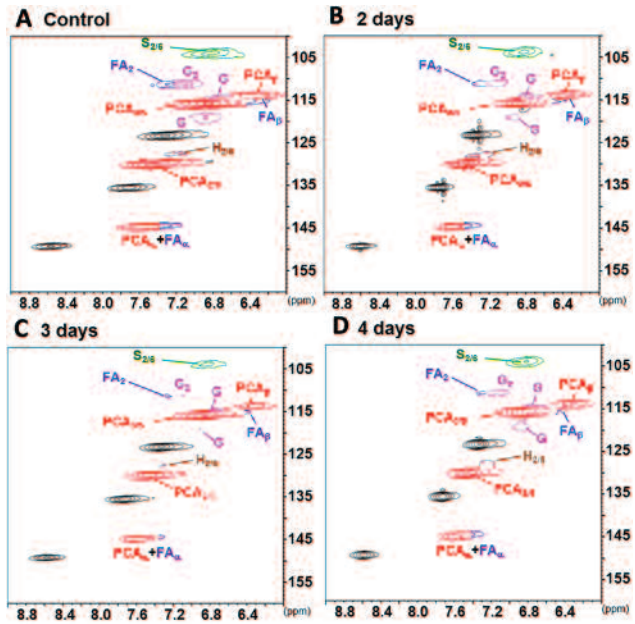

Fig. 7 Expanded HSQC NMR spectra in aromatic region (δ_C/δ_H 100–160/6.0–9.0 ppm) of solid residues before and after enzyme treatments for 2–4 days with non-dialyzed secretome. (A) DMR-EH control (autoclaved) without enzyme, (B, C, D) 2, 3, and 4 days of treatment with *P. eryngii* secretome containing 30 U laccase per g.

β-O-4 leveled-off after 3 days. The methoxyl peak at δ_C/δ_H 54–57/3.1–4.5 ppm also decreased, indicating that demethoxylation occurred, likely catalyzed by laccase.

C1 anomeric peaks in sugar at δ_C/δ_H 93/5.05, 98/4.45 and 108/5.5 ppm disappeared in the control, suggesting that 4-O-Me-glucuronic acid units and 2-O-Ac-β-D-xylopyranose units were solubilized without the secretome, potentially during autoclaving. The peak intensities of C6 in cellulose at δ_C/δ_H 60/3.4 ppm and xylan peaks at the region of δ_C/δ_H 58–80/2.9–4.6 ppm slightly decreased for longer treatments. Anomeric peaks in cellulose and xylan at 102/4.4 ppm exhibit a similar trend to xylan peaks. These results show that carbohydrates in DMR-EH lignin were slightly depolymerized by the fungal secretome (as corroborated by the presence of some carbohydrate-active enzymes shown below *via* proteomics).

Expanded HSQC spectra in the aromatic region are shown in Fig. 7. The types of subunits (S, G, PCA, and FA) in Fig. 7 are the same as in Fig. 2B. All of the correlation peaks in the DMR-EH control are similar to those in DMR-EH lignin, demonstrating that the lignin aromatic structure was not significantly altered by autoclaving and the incubation of the substrate without the secretome. Peaks of S2/6 and G2/5/6 decreased in 3 days, but slightly increased at 4 days. The peak for PCA2/6 also decreased somewhat at 2 days and did not change at 3 and 4 days. The FA peak decreased considerably at 2, 3, and 4 days. These results suggest that the repolymerized portion at 4 days probably consisted of G and S units, and that PCA was slightly reduced although FA was almost fully absent. It is noteworthy that Cα-OH is often oxidized by laccase and subsequently the Cα–Cβ bond is cleaved to generate aldehyde, carboxylic acid, and quinone structures. However, there are no correlation peaks of aromatic-C2/6 in Cα-oxidized S-type lignin unit at δ_C/δ_H 106.1/7.31. Also, no peaks of aldehyde and carboxylic acid were detected in the ^{13}C-NMR spectrum. This result implies that generated intermediates of aldehydes and quinones repolymerized, which is in agreement with an increase in M_w in 4 days.

In conclusion, these data suggest how the laccase-rich *P. eryngii* secretome depolymerizes lignin, but also how a repolymerization effect takes place at the end of these treatments in the assay conditions. On the basis of these results, we selected 3 days and 30 U g^{-1} as optimum treatment length and laccase dosage, respectively, to obtain the highest depolymerization extent in further experiments.

Testing the "microbial sink" hypothesis: incubation of an aromatic catabolic bacterium and the *P. eryngii* secretome to enhance DMR-EH lignin depolymerization

The results in Fig. 5 suggest that LMW lignin is being repolymerized during the end of the enzyme treatments. As such, the next experiment was designed to combine an aromatic catabolic bacteria and fungal enzymes to potentially avoid repolymerization of monomeric species and/or increase the lignin depolymerization degree. We dub this hypothesis the "microbial sink", wherein a microbe catabolizes aromatic com-

pounds while ligninolytic enzymes depolymerize lignin. To test this concept, it is essential to monitor changes in lignin (*e.g.*, GPC) and microbial growth (OD_{600}). When mixed physically together, bacteria often stick to biomass, thus potentially causing interference and leading to poor results for both GPC and OD_{600} measurements. As such, bacteria were cultivated in a dialysis membrane with DMR-EH lignin and fungal enzymes added external to the membrane. The dialysis membrane cutoff was <3.5 kDa, such that only small molecules and no proteins could pass through.

Control experiments were first conducted to test the resistance of the cellulose-based dialysis membranes to the fungal secretome as cellulases in either the secretome or secreted by *P. putida* could compromise the membrane integrity. In addition, several cellulase assays were performed in the secretome, and no activity was detected in the assay conditions. Simultaneously in this control experiment, we demonstrated that LMW compounds were able to pass through the membrane to serve as a carbon and energy source for *P. putida* by adding glucose outside the membrane as the sole carbon and energy source; in this experiment, the bacteria grew to an OD_{600} of 6 and the membrane conserved its integrity.

After demonstrating both the resistance and permeability of the membrane, we conducted experiments with (1) DMR-EH and boiled (inactivated) fungal secretome, (2) DMR-EH and active fungal secretome, (3) DMR-EH, inactivated fungal secretome, and membranes with bacteria, and (4) DMR-EH, active fungal secretome, and membranes with bacteria (Fig. 8A). The secretome used for these experiments was dialyzed to avoid interference with the fungal growth media. Bacterial growth was analyzed at the end point of the experiment (3 days). Bacterial ODs were higher in the samples containing the active secretome (OD = 5.2 ± 0.2) (Fig. 8B) than those ones with the inactivated one (OD = 4.3 ± 0.6). In addition, Fig. 8B also shows that the membranes appear clean after the cultivations, suggesting no major issues with lignin adsorption to the membranes. Fig. 8C shows the M_w of DMR-EH lignin in the insoluble and soluble fraction after each treatment. The M_w

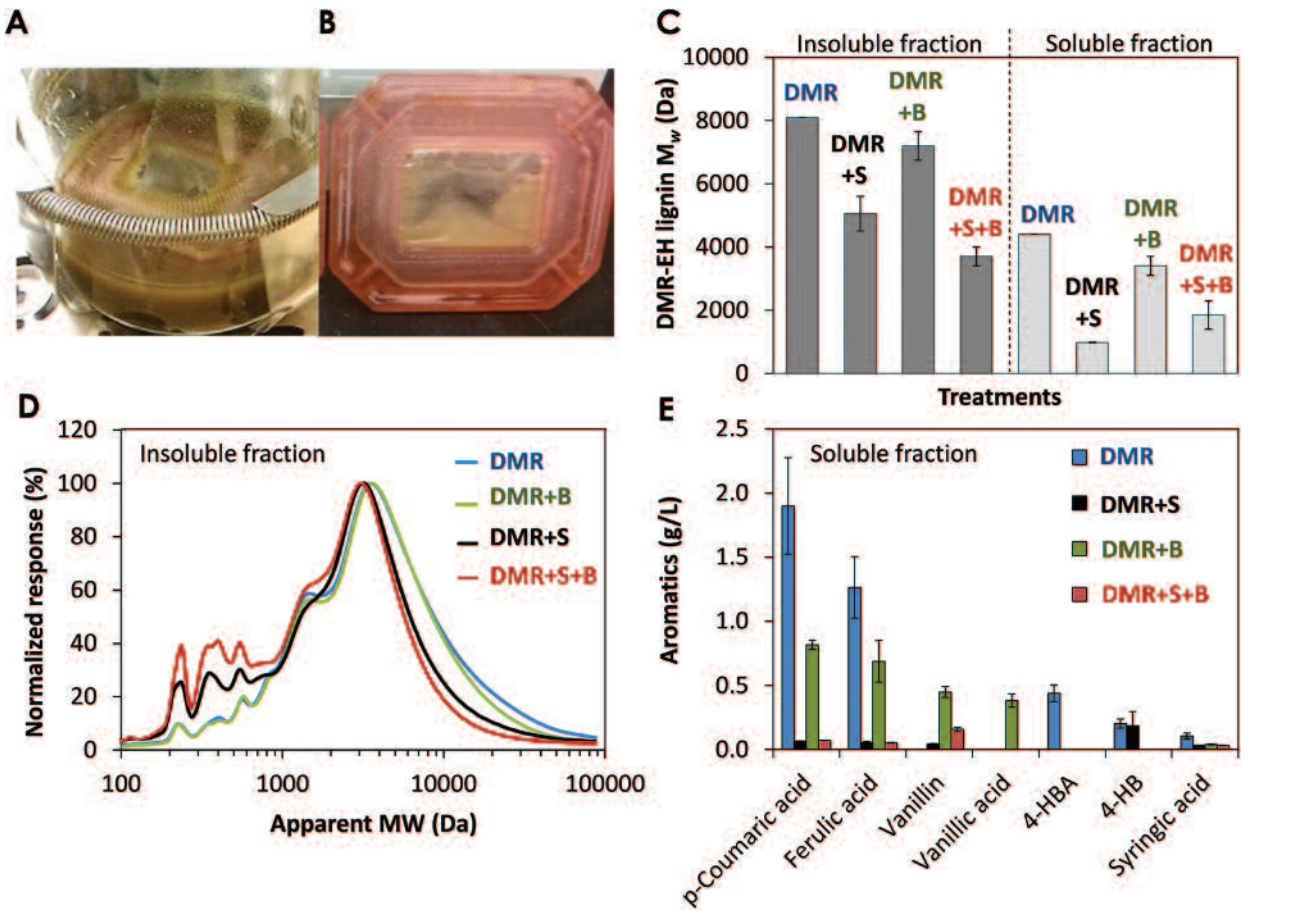

Fig. 8 Incubation of DMR-EH lignin, the *P. eryngii* secretome, and *P. putida* KT2440 to demonstrate the microbial sink concept. (A) DMR-EH with fungal secretome and bacteria. (B) Bacterial growth after the treatment represented in (A). (C) DMR-EH lignin M_w obtained from the different treatments in the insoluble and soluble fractions. (D) GPC profiles of DMR-EH lignin from the insoluble fraction after the different treatments. (E) LC-MS/MS from the soluble fraction at the end point of the different treatments. DMR = DMR-EH with inactivated fungal secretome; DMR + S = DMR-EH with fungal secretome; DMR + B = DMR-EH with bacteria and inactivated secretome; DMR + S + B = DMR-EH with bacteria and fungal secretome; 4-HBA: 4-hydroxybenzoic acid; 4-HB: 4-hydroxybenzaldehyde.

decreased significantly after adding the fungal secretome, 38% in the solid and 78% in the liquid fraction. However, when adding the membrane system with both *P. putida* KT2440 and the secretome (DMR + B + S), the decrease was more pronounced for the solid fraction at 55%, but not for the liquid fraction (58%). These results demonstrate that if bacteria are present, the lignin depolymerization extent increases; however, in the liquid fraction, the lower apparent extent of M_w decrease is likely a result of the catabolism of LMW species (the microbial sink) thus leading to an increase in the apparent M_w of that fraction due to bacterial removal of catabolized species. A minor reduction of the M_w of insoluble lignin was also observed when having only bacteria (~12%) (Fig. 8C); however, the GPC profile shows (Fig. 8D) how the LMW lignin is not released in that case, as it does in the presence of ligninolytic enzymes. Table S3† shows different GPC parameters from these results. It is also worth noting here that the solubilization degree of DMR-EH was similar after all the treatments (~40%) as well as the lignin content in the insoluble fraction (~41%) (data not shown). These results show that although substrate *solubilization* (into water) is not enhanced after the enzyme and/or bacterial treatment, depolymerization of HMW lignin is prevalent (Fig. 8C).

To determine if bacteria are consuming aromatic compounds, LC-MS/MS was performed in the soluble fraction from all the treatments, and seven aromatic species were abundant (Fig. 8E). It is evident that some monomeric aromatics, such as PCA, FA, 4-hydroxybenzoate, and syringate, decrease and/or disappear in the presence of the secretome alone and in the presence of bacteria alone. This observation demonstrates how the enzymes in the secretome can act on these monomeric compounds, but also how the bacterium consumes the aromatic compounds, respectively. In addition, vanillin and vanillate appear primarily in the treatments where bacteria are present and not in the control (DMR-EH). These aromatic compounds are intermediates in the catabolism of FA with vanillate being a typical bottleneck in this pathway in *P. putida* KT2440.[27] The presence of vanillin in the DMR + S + B soluble fraction demonstrates how catabolism may be more rapid than the secretome enzymatic action on the LMW aromatic compounds present in the soluble fraction. Lastly, 4-hydroxybenzaldehyde (4-HB), which is present in the control, is also metabolized by *P. putida* KT2440; however, it is not a substrate for ligninolytic enzymes (Fig. 8E). Overall, the presence of a microbial sink appears to enhance the overall extent of lignin depolymerization.

Proteomic analysis of *P. eryngii* secretome

The current work demonstrates how the *P. eryngii* secretome is able to depolymerize lignin from the solid DMR-EH stream. Among the enzymes analyzed, there may be isoenzymes that exhibit similar activities or enzymes not detected at the assay conditions. Consequently, to more deeply characterize the enzyme cocktail utilized in the current study, a proteomic analysis was performed. Over 400 proteins in the *P. eryngii* secretome were classified after BLAST searches[39] against a combination of Uniprot and NCBI (fungal kingdom) to obtain the best hit (defined as the match with the lowest *E*-value and highest percent identity) and non-hypothetical match. The first non-hypothetical match was the one considered to classify the proteins (Fig. 9). To determine the relative abundance of the proteins, the sum of the peptide spectrum matches (PSMs) belonging to each protein were utilized. Only those proteins with ≥2 peptides detected were considered in the analysis.

Proteins were first organized by function and abundance (Fig. 9A). The oxidoreductase group was the most abundant (38%) despite containing a fewer number of proteins than the Glycoside Hydrolases (GHs) (42 and 82 proteins, respectively). GHs (23%) are the second most abundant group followed by proteinases (11%) and esterases (5%) (Table S4†). As oxidoreductases are the main proteins involved in lignin depolymerization, a deeper analysis of this group is also presented (Fig. 9B, Table S4†). Glucose/methanol/choline (GMC) oxidoreductases (41%), AAOs (14%) (which are also GMC-oxidoreductases), and laccases (23%) were the most abundant oxidoreductases, comprising 78% of the total. It is also noteworthy that peroxidases (*e.g.*, DyP-type peroxidases, 4%) were quite limited in number in the 9-day fungal secretome, which matches with the low measured peroxidase activities (Fig. 3D). The presence of a signal peptide cleavage site, which predicts if a protein could be secreted, was also analyzed in these 42 oxidoreductases. Only 8 proteins did not contain a signal peptide, namely one DyP, the two reductases, the three FMN-linked oxidoreductases, one glyoxal oxidase, and one AAO

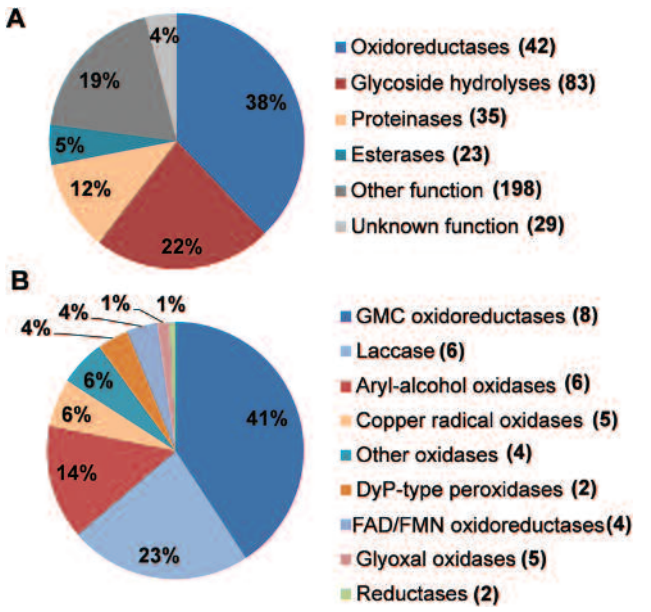

Fig. 9 Proteomic analysis of the secretome of *P. eryngii* utilized for DMR-EH lignin depolymerization assays. (A) Functional classification of the proteins detected in the fungal secretome. (B) Classification of the oxidoreductases in the secretome. The abundance of each group, calculated by the sum of the PSMs belonging to each protein, is presented as a percentage. The numbers in parentheses at the right side of each protein group indicate the number of different proteins observed.

(Table S4†). Although proteins with one unique peptide were not considered for the analysis, it is noted that a single peptide was also found for an unidentified heme-peroxidase and a short MnP (data not shown).

Regarding the composition of the second major functional group, GHs, proteins such as cerato-platanins, α-L-arabinofuranosidases, glucoamylases, GH family 79 (which contains proteins such as β-glucuronidases), and 1,3-β-glucosyltransferases (Table S4†) were the most abundant. It is worth mentioning that in this group, three hits for the GH Family 61 were also found. Although they are included in GH category, according to their current characterized function,[40] GH61s are lytic polysaccharide monooxygenases. Overall, the oxidoreductases are the most prevalent group of enzymes in this organism which aligns well with its ability to selectively depolymerize lignin in biomass.[41]

Discussion

Selective and efficient lignin depolymerization remains one of the main challenges in biomass conversion. Currently, lignin upgrading to value-added compounds, such as polyhydroxyalkanoates, fatty acids, or muconic acid, has been described, but primarily from LMW lignin species.[7,27,28,42] Although advances have been made in the lignin depolymerization field by bacteria,[4,7,43] carbon conversion remains low. Fungal ligninolytic enzymes, on the other hand, are effective at depolymerizing lignin and could be a powerful complement to enhance bacterial lignin conversion. However, these types of enzymes are also involved in lignin polymerization,[12,16] which could limit monomer yields. Thus, from another perspective, bacteria could be also considered a natural "microbial sink" to minimize action of ligninolytic enzymes on LMW compounds.

In the current study, a biorefinery stream, DMR-EH lignin, was utilized to demonstrate how fungal ligninolytic cocktails can depolymerize lignin and to test how bacteria can enhance the resulting depolymerization. Typically, most *in vitro* studies utilizing oxidoreductases to depolymerize lignin employ commercially available single enzymes, not secretomes. The content of a "ligninolytic cocktail" is highly dependent on the fungus, as demonstrated in Fig. 3, but also on the culture conditions.[9,44] Here, a standard medium for white-rot fungal cultivation was used, but supplemented with autoclaved DMR-EH since lignocellulosic substrates induce production of ligninolytic[9] and cellulolytic enzymes.[10] The fungi *P. eryngii* and *Bjerkandera* sp. were chosen from an initial screening with the highest laccase and peroxidase activity, respectively. Moreover, a specific harvesting time was selected that exhibited primarily one enzyme activity or the other (especially in *P. eryngii*). The secretion of these enzymes by these fungi has been reported previously[45,46] and trends, in particular for laccase production, are similar to those found earlier.[45] However, the secretomes from these fungi have never been utilized for lignin depolymerization. In fact, the few studies reporting the use of fungal secretomes are more related with the production of mechanical pulps and the improvement of their properties.[47] In addition, in the pulping field, delignification is measured by the decrease of the kappa number;[48] however, with this type of analysis, it is difficult to know if lignin depolymerization is occurring or if it is just a grafting effect mediated by laccases that modifies lignin and enhances solubility.[12]

Regarding substrate conditioning, DMR-EH was subjected to different processing as required prior to each enzyme treatment (*i.e.* with and without autoclaving, different pH, and different buffers). These variations changed the M_w of lignin. For instance, a M_w of 6100 Da (Fig. 4B), 5500 Da (Fig. 5D), and 8000 Da (Fig. 8C), all at pH 7, were observed for the insoluble (non-enzyme treated) fraction of non-autoclaved, autoclaved with malonate buffer, and autoclaved with phosphate buffer samples, respectively. Moreover, when pH 4.5 in non-autoclaved DMR-EH was used, a M_w of 12 000 Da (Fig. 4A, C and D) was measured. These results show that lignin solubilization is highly dependent on pH, with the M_w of DMR-EH lignin at pH 7 being ~50% lower than at pH 4.5. Conversely, during autoclaving, lignin can also likely undergo additional polymerization, increasing the initial M_w. As such, the pH and DMR-EH conditioning are critical for the current experiments.

Fungal ligninolytic enzymes generally have low optimal pH (<5), in particular peroxidases; on the other hand, the aromatic-catabolizing bacteria (*P. putida*) used in the current study grows optimally at pH 7. As such, we performed depolymerization assays at pH 4.5 and 7. Although the degree of depolymerization was maximum when using mixed *P. eryngii* and *Bjerkandera* secretome at the highest enzyme dosage at pH 4.5 (around 84%) (Fig. 4D), the final lignin M_w was similar to that obtained in treatments with the *P. eryngii* secretome (30 U laccase per g) at pH 7 (Fig. 3B) at 2300 Da. This M_w roughly corresponds to oligomers of 10 units of aromatics, a considerable reduction of the M_w of the solid fraction when compared with the initial DMR-EH substrate M_w (10 000 Da) (Fig. 2A). Around 50% M_w reduction was reached just with the pH adjustment, which increased to 75% upon addition of the secretome. Considering these results, the laccase-rich secretome was selected over the peroxidase-rich enzyme cocktail for reasons mentioned above. Nevertheless, laccases are not typically able to oxidize non-phenolic compounds if mediators are not present. However, aromatic compounds such as sinapic acid, PCA, and FA are natural mediators that increase the ability of laccases to oxidize more recalcitrant compounds.[49,50] As presented in Fig. 8E, PCA and FA are the main aromatic compounds detected in the supernatant of DMR-EH lignin, and thus, laccases could use these as mediators to enhance their substrate oxidation abilities.

Compiling results from the published work using ligninolytic enzymes on lignin-rich substrates, it is apparent that depolymerization is highly variable, making direct comparisons difficult, considering the diversity of substrates and the different lignin analysis methodologies employed. For pure peroxidase treatments, for example, a horseradish peroxidase (HRP),[51] fungal LiPs and MnPs from *P. chrysosporium*,[52] and VP from *P. eryngii*[53] have been tested and demonstrated some

degree of lignin depolymerization on different substrates such as synthetic lignin, insoluble isolated poplar lignin, and lignosulfonates, respectively. Recently, a laccase from *Myceliophthora thermophila* and *Trametes villosa* were utilized to delignify eucalyptus.[13,22,23] In this case, Cα–Cβ cleavage was demonstrated, but the molecular weight changes were not reported. Instead, in this case, a reduction in the Klason lignin content was evident. Nevertheless, different to our work, those enzyme treatments were complemented with peroxide, which also could enhance lignin degradation. Laccase dosage has been also presented as another important parameter to improve the depolymerization degree (Fig. 4 and 5). Chen *et al.*[54] utilized laccase in synergy with cellulases demonstrating lignin decomposition and increasing sugar yields at a dosage of 4000 U g^{-1} of material. The highest dosage utilized in the current study is 100 U g^{-1} at pH 4.5, thus complicating direct comparisons.

Many studies utilizing pure laccases to oxidize substrates also supplement mediators (natural or synthetic) to enhance lignin depolymerization.[55] However, it is not still clear if these mediators can also increase lignin polymerization.[56] Both depolymerization and repolymerization processes are natural effects produced *via* free radical generation by oxidoreductases.[12] In the time course experiment shown in Fig. 5, repolymerization was observed from 3 to 4 days at all the enzyme dosages and using dialyzed and non-dialyzed secretomes. Hofrichter *et al.* reported that a MnP from *Phebia radiata* polymerized and depolymerized according to the initial nature of the substrate, LMW and HMW lignin, respectively.[57] As this work is performed with an entire secretome and not a single enzyme, it is challenging to pinpoint the main factor responsible for this effect. The nature of the substrate is likely to partially determine these responses, although the literature is not clear. For instance, HRP and laccase treatments in milled wood lignin solubilized in NaOH mainly resulted in depolymerization;[58] however, some efforts in industrial lignin (from a paper factory and also solubilized in NaOH) with semi-purified laccase from *Fusarium proliferatum* exhibited considerable polymerization, but when ABTS was used as a mediator, depolymerization was also observed.[59]

The search for a "radical sequestration" agent could be an alternative to decrease the degree of repolymerization. Dordick *et al.*[51] reported that peroxidases depolymerize lignin only in organic media, but not water, highlighting that solvents might quench free radicals that lead to repolymerization. Also, the presence of enzymes such as AAO (synonym: veratryl alcohol oxidase) from *P. ostreatus* have been described to prevent polymerization in substrates oxidized by laccases by reducing aromatic radicals.[9,60] These type of oxidases are also involved in providing H_2O_2 to peroxidases. In the secretome utilized here, AAOs are present (Fig. 3D and 9B), which could have a similar effect and, indirectly, improve depolymerization. However, the main radical sequestration in the current study is likely to be the microbial sink. Results presented in Fig. 8 demonstrate how the treatment with both the *P. eryngii* secretome and bacteria increase the depolymerization degree compared to those treatments alone. The GPC chromatogram of the solid fraction (which shows a M_w reduction greater than 50% compared to control), LC-MS/MS of soluble fraction (showing the presence of bacterial aromatic intermediates that are not present in the control), and bacterial growth into the membranes (higher when the secretome is also present), all support the idea of the bacteria taking up aromatic compounds and improving depolymerization of DMR-EH lignin. A similar study was performed utilizing the secretome from the fungus *P. chrysosporium* (with high peroxidase content instead of laccases) and the bacterium *Xanthomonas* sp. by using different M_w lignins.[61] However, in this case, after adding the secretome, lignin mineralization by the bacteria was lower likely due to an increase in the M_w of lignin and thus, being less available for the bacterium. Another recent study also utilized a pure laccase cocktail from *T. versicolor* and the bacterium *Rhodococcus opacus* during Kraft lignin degradation; however, lignin M_w (analyzed by GPC), also increased in all cases.[42]

As highlighted above, lignin depolymerization by *P. eryngii* secretome cannot be only attributed to the presence of laccases but the synergy of all the proteins secreted. Thus, to obtain a deeper characterization of the enzyme cocktail utilized, a proteomics study of the fungal secretome was also conducted. As expected, due to the selective nature of this fungus for depolymerizing lignin, the major functional group was the oxidoreductases (Fig. 9A). Apart from laccases, GMC oxidoreductases were also a major enzyme family present in the secretome. Considering previous enzymatic studies on *P. eryngii*, the activity of the GMC enzymes in this organism are hypothesized to possess an AAO activity.[62] As expected, GHs were also detected in the secretome. Considering that typical biorefinery streams would contain polysaccharides and lignin, the use of complete fungal secretomes could have the advantage of enhancing substrate degradation and thus improving final carbon availability and conversion. A proteomic study has been recently performed in the fungal counterpart *P. ostreatus.*[9] In that study, 508 proteins were detected after 21 d cultivation. Here, we are presenting a fungal cocktail of over 400 proteins detected after 9 days of incubation in the presence of DMR-EH. The number of proteins reported in these studies highlights how complex lignocellulose degradation is in Nature and how potentially difficult relying on a single enzyme will be for efficient lignin depolymerization.

Conclusion

As demonstrated in this work, fungal secretomes containing high laccase and peroxidase activity are able to depolymerize a solid lignin-rich substrate with native lignin like properties. In addition, a new concept dubbed the "microbial sink" is presented which is based – as it could occur in Nature – on complementing fungal ligninolytic enzymes and an aromatic-catabolizing bacterium. This "natural synergy" might act as a sequestration mechanism to avoid the repolymerization of

LMW lignin *via* enzyme redox reactions, thus improving lignin depolymerization. Despite partial depolymerization of solid lignin using a solely biological approach, higher lignin conversions will be required for realistic lignin valorization processes. In future work, we will report chemo-catalytic solubilization of the DMR-EH residual lignin, which may enable higher extents of microbial lignin conversion.

Materials and methods

Substrate preparation

Corn stover was deacetylated and mechanically disc refined at 1 ton per day pilot plant scale according to Chen *et al.*[63] Enzymatic digestions were carried out using NREL's 1900-L DI paddle mixer. The 1900-L DI mixer was cleaned and sterilized at ~120 °C–130 °C for 1 h prior to adding 268 kg (110 kg dry) of DMR corn stover and the ~30 wt% slurry was pasteurized at 80 °C for 2 h. The pH of the slurry was adjusted to 5.0. The remainder of the water was added and the pH adjusted to 5.0 at 50 °C prior to adding the cellulase and hemicellulase enzyme preparations to give a final total solids loading of ~20 wt%. The enzyme loading was 50 mg Novozymes CTec3 per g of glucan and 10 mg HTec3 per g xylan in the DMR residues. The temperature was maintained at 48–50 °C for 3 days. The liquor was drained and washed to remove residual components. The solids were further enriched in lignin by repeating the enzymatic hydrolysis to remove more of the glucan and xylan in similar conditions along with adding 1 μg L^{-1} of Lactrol (Phibro) to inhibit microbial contamination. The solids were washed three times with water and centrifuged at 8000*g* for 30 min. The supernatants were then decanted and the remaining solids were lyophilized for storage and further characterization.

Substrate characterization

Full compositional analysis. Compositional analysis was performed according to the procedure in NREL LAP/TP-510-42618[64] to determine lignin, sugar, and other organic compound concentrations in the substrate.

Gel permeation chromatography (GPC) analysis. DMR-EH residue (20 mg) was acetylated in a mixture of pyridine (0.5 mL) and acetic anhydride (0.5 mL) at 40 °C for 24 h with stirring. The reaction was terminated by addition of methanol (0.2 mL). The acetylation solvents were then evaporated from the samples at 40 °C under a stream of nitrogen gas. Samples were further dried in a vacuum oven at 40 °C overnight. The dried, acetylated samples were suspended in tetrahydrofuran (THF, Baker HPLC grade), and then filtered through 0.45 μm nylon membrane syringe filters. Most of lignin in the samples was soluble in THF as measured by ^{13}C solid-state NMR of the insoluble material, but polysaccharides were not fully acetylated and not dissolved in THF. GPC analysis was performed using an Agilent HPLC with 3 GPC columns (Polymer Laboratories, 300 × 7.5 mm) packed with polystyrene-divinyl benzene copolymer gel (10 μm beads) having nominal pore diameters of 10^4, 10^3, and 50 Å. The eluent was THF and the flow rate 1.0 mL min^{-1}. An injection volume of 25 μL was used. The GPC was attached to a diode array detector measuring absorbance at 260 nm (band width 80 nm). Retention time was converted into molecular weight (MW) by applying a calibration curve established using polystyrene standards. The highest response value in the *y*-axis in each GPC chromatogram was normalized to 100.

NMR. HSQC NMR spectra were acquired for DMR-EH. DMR-EH (0.2 g) was ball milled by a planetary ball milled using a Retsch PM100 mill fitted with a 50 mL ZrO_2 grinding jar and 10 × 10 mm ball bearings, set at 600 rpm. Ball milled DMR-EH (80 mg) was suspended into d_6-DMSO/d_5-pyridine (4 : 1, v/v) in a NMR tube. The mixture was sonicated for 5 h until the gel became homogeneous.[32]

Spectra were acquired at 40 °C on a Bruker Avance III 600 MHz spectrometer at 11.7 T using a TCI cryoprobe. Spectra were acquired with 1024 points and a sweep width of 15 ppm in the F2 (^1H) dimension and 512 points and SW = 220 ppm in the F1 (^{13}C) dimension. Peak assignment was performed according to literature.

Analysis of aromatics by LC-MS/MS. Mass spectrometry was used in the last experiment of the current study to analyze aromatics from the soluble fraction. For this purpose, 14.5 mg of freeze-dried supernatant from 8 different treatments was reconstituted in 1 mL methanol. Analysis of samples was performed on an Agilent 1100 LC system equipped with a diode array detector (DAD) and an Ion Trap SL MS (Agilent Technologies, Palo Alto, CA) with in-line electrospray ionization (ESI) as detailed in the ESI.† Vanillin, 4-hydroxybenzaldehyde, PCA, vanillic acid, syringic acid, 4-hydroxybenzoic acid, and FA were the only aromatics detected from an instrument specific in-house database of 70 aromatic compounds. Standards were prepared in the range of 1–100 μg mL^{-1} and run at the same conditions as the samples.

Fungal strains and cultivation conditions

The strains of basidiomycetes used in the present study were obtained from Centraalbureau voor Schimmelcultures (CBS; Baarn, The Netherlands) and Instituto Jaime Ferrán de Microbiología (IJFM; Centro Investigaciones Biológicas, Madrid, Spain). The fungal species consisted of *Bjerkandera* sp. IJFM A660, *Bjerkandera adusta* CBS 230.93, *Cerioporopsis subvermispora* IJFM A718, *Irpex lacteus* IJFM A792, *Panus tigrinus* IJFM A768, *Phanerochaete chrysosporium* CBS 481.73, *Phellinus robustus* IJFM A788, *Pleurotus eryngii* IJFM *A582*, *Pleurotus ostreatus* CBS 411.71, *Polyporus alveolaris* IJFM A794, *Stereum hirsutum* IJFM A793, and *Trametes versicolor* IJFM A136. Strains were maintained on 2% malt extract agar (w/v) and preserved at 4 °C. With the aim of reviving the fungi before starting the experiments, fungi were individually cultured at 28 °C for 7 days on potato dextrose agar (39 g L^{-1}) plates. After this incubation time, four agar plugs of about 1 cm^2 were cut from actively growing mycelium and inoculated into 250 mL Erlenmeyer baffled flasks with 50 mL of modified Czapek-Dox media (final pH 5.9), which contained 10 g L^{-1}

glucose, 2 g L^{-1} ammonium tartrate, 1 g L^{-1} KH_2PO_4, 0.5 g L^{-1} $MgSO_4 \times 7{\cdot}H_2O$, 0.5 g L^{-1} KCl, 1 g L^{-1} yeast extract, 5 g L^{-1} peptone, 0.1 g L^{-1} $B_4O_7Na_2 \times 10{\cdot}H_2O$ and 1 mL L^{-1} of trace elements which contained (×1000) 16 mg L^{-1} $MnSO_4$, 27 mg L^{-1} Fe_2SO_4, 74 mg L^{-1} $CuSO_4 \times 5{\cdot}H_2O$, and 73 mg L^{-1} $ZnSO_4 \times 7{\cdot}H_2O$. After 6 days of incubation at 28 °C and 180 rpm, each culture was aseptically blended (Bead Beater) for 30 seconds to homogenize mycelia size, and 2.5 mL (per 50 mL of media) were used to inoculate those flasks for the enzyme screening and secretome production.

Enzyme screening in fungal secretomes

To determine the best fungal species producing ligninolytic enzymes, an initial screening was performed in the secretome of twelve basidiomycetes (detailed above) while growing in the presence of DMR-EH lignin. For this purpose, triplicates of 250 mL flasks containing 50 mL of modified Czapek-Dox growth media and 1% DMR-EH were utilized to grow each strain. Fungi were incubated at 28 °C and 180 rpm during 15 days. Samples (1 mL) were taken every two days since the third day during the whole incubation time. Samples were then centrifuged during 10 minutes at 14 000 rpm and the supernatant transferred to another tube for further enzyme assays.

Enzyme assays

Different UV/colorimetric enzyme assays were performed in the fungal supernatants to evaluate activities such as laccase, AAO, MnP, DyP, LiP, and other peroxidases such as VP. Laccase activity was determined following ABTS oxidation to its cation radical (ε_{418} = 36 000 cm^{-1} M^{-1}) in 100 mM tartrate buffer at pH 5. AAO activity was assayed by veratraldehyde formation from 5 mM veratryl alcohol in 100 mM sodium tartrate buffer at pH 5 (ε_{310} = 9300 cm^{-1} M^{-1}). MnP and VP activity can be measured by the formation of Mn^{3+}–tartrate complex (ε_{238} = 6500 cm^{-1} M^{-1}) during the oxidation of 0.1 mM $MnSO_4$ in 100 mM tartrate buffer at pH 5. LiP activity was assayed by veratraldehyde formation from 5 mM veratryl alcohol in 100 mM sodium tartrate buffer at pH 3 (ε_{310} = 9300 cm^{-1} M^{-1}). Other peroxidase activities such as DyP and short-MnP could be also followed by the oxidation of ABTS in the absence and the presence of 0.1 mM $MnSO_4$ at pH5 respectively. VP can be detected using ABTS as well with and without Mn^{2+}. In all cases, peroxidase activity assays were conducted in the presence of 0.1 mM H_2O_2 excluding LiP, which was activated by 0.4 mM H_2O_2. Peroxidase activities evaluated through ABTS were all corrected by subtracting laccase activity. The discoloration of reactive blue 19 (anthraquinone dye) at 50 μM (ε_{595} = 10 000 cm^{-1} M^{-1}) and reactive black 5 at 25 μM (ε_{598} = 30 000 cm^{-1} M^{-1}) in sodium tartrate buffer at pH 4 were also used to ascertain the type of peroxidase, being VP able to discolor reactive black 5 and DyP both of them in the presence of 0.1 mM H_2O_2. One enzymatic activity unit was defined as the amount of enzyme that oxidizes 1 μmol of substrate in 1 min.

After the enzyme screening, both laccases from *P. eryngii* and peroxidases from *Bjerkandera* sp. were tracked by ABTS oxidation at pH 4.5 and 7 in 100 mM sodium malonate. Peroxidases were tested in the absence and the presence of 0.1 mM $MnSO_4$ and activated by 0.1 mM H_2O_2. The buffer was selected based on the buffering capacity at that pH range and its manganese chelating properties. Laccases from *P. eryngii* were evaluated in the last experiment in phosphate buffer at pH 7 instead of sodium malonate since that was the main buffer during the depolymerization assay. Laccase activity in both buffers was similar.

The secretome of *P. eryngii* was also evaluated for cellulase activity by measuring the activity on amorphous and crystalline cellulose.[65] 500 μg of secretome proteins were mixed in a 1% slurry of cellulose substrate and incubated at 28 °C for 5 days in a rotisserie incubator. The mixture was then run on an HPLC and no measurable levels of cellobiose, glucose, or xylose were detected.

Secretome production and processing

To produce larger secretome volumes from the selected fungi, 1 L flasks containing 200 mL of modified Czapek-Dox media and 1% DMR-EH were selected to grow the fungi. Cultures were incubated at 28 °C and 180 rpm, enzymes evaluated every day, and secretomes collected after 9 days. To process the secretome, cultures were filtered through Miracloth to remove the fungi, then through 1.1 μM pore size glass fiber filters, and lastly through 0.2 μM pore size PES filters (Thermo Scientific™ Nalgene™ Rapid-Flow™) in sterile conditions.

For the last experiments with the *P. eryngii* secretome, part of the secretome was dialyzed in a 350 mL pressurized ultracentrifugation system (Amicon) with 10 kDa membranes. In detail, at least 1 L of secretome broth was concentrated down to approximately 40 mL and then washed several times with saline buffer until the dialysis factor was higher than 100. The dialysis buffers depended on the subsequent experiment. For the depolymerization assays over time with the *P. eryngii* secretome, 20 mM sodium malonate at pH 7 was used. For the experiment where bacteria were present, 20 mM phosphate at pH 7 (Na_2HPO_4 and KH_2PO_4 at a ratio of 1 : 2.2) was utilized. The volume of the dialyzed secretomes was adjusted to achieve the same laccase activity values than in the original, non-dialyzed secretome.

Enzyme depolymerization assays of DMR-EH

DMR-EH treatment with the secretome of *P. eryngii* and *Bjerkandera* sp. at pH 4.5 and pH 7. Before starting the depolymerization assays, laccase and peroxidase activity was measured at pH 4.5 and 7 using ABTS as substrate, and peroxidase activity calculated in the presence of Mn^{2+} and H_2O_2 as previously described. Laccases from *P. eryngii* were active at both pHs but the peroxidases from *Bjerkandera* only at pH 4.5. Thus, treatments with the *P. eryngii* secretome were carried out at both pHs, but treatments containing peroxidases from the *Bjerkandera* secretome only at 4.5. The pH was tracked during the incubation time, and no changes were observed. Regarding enzyme stability, laccase and peroxidase activity remained at the end of the treatments.

Different volumes from both fungal secretomes were utilized to achieve different laccase and peroxidase dosages at the different pHs. The enzyme added in each treatment was expressed as total U per gram of DMR-EH. We evaluated laccase at dosages of 10, 50, and 100 U g^{-1} at pH 4.5 and 3, 15, 30 U g^{-1} at pH 7 and peroxidase from *Bjerkandera* sp. at dosages of 8, 40, 80 U g^{-1} at pH 4.5. Secretomes were added to 250 mL flasks containing 0.5 g DMR-EH, 10 mL sodium malonate (250 mM) at pH 4.5 or 7, and 150 μL of tetracycline (250 μg mL^{-1}) to avoid bacterial contamination. Sterile distilled water was also added to achieve a total volume of 50 mL. When the secretomes of both fungi were complemented, half volume of each secretome was utilized. In addition, in those treatments using *Bjerkandera*'s secretome, 0.1 mM $MnSO_4$ and 0.5 mM H_2O_2 were also included, the latter added at 0, 4, 8, 12, 22, 28, 34, 48, 54, 60, 72, 78, 84, 96, 104, 120, 128 h. The same H_2O_2 concentration was selected across each enzyme loading since the exact amount of peroxidase (mg mL^{-1}) in the sample and the abiotic effect of H_2O_2 on the lignin were unknown. Control treatments without enzyme addition were carried out in parallel at both pHs and in the presence and the absence of $MnSO_4$ and H_2O_2 and analyzed after 6 days of incubation. Treatments were performed at 30 °C, 150 rpm during 3 and 6 days, although at 3 days only those treatments utilizing the highest enzymes dosages were sampled. After incubation, the flask content was centrifuged at 5000 rpm for 20 min. The supernatant was collected and the solid fraction weighted after drying at 60 °C for 48 h. This solid fraction was then utilized for GPC analysis.

DMR-EH treatment with the secretome of *P. eryngii* at pH 7 over time. Considering the results obtained in the previous experiment, the treatment with the *P. eryngii* secretome at pH 7 was the selected condition to obtain DMR-EH lignin with the lowest molecular weight. For a time-dependent characterization of depolymerization, three different enzyme dosages were utilized (3, 10, 30 U laccase per g DMR-EH) and GPC analysis were performed from samples collected over time. The secretome utilized for this experiment was both dialyzed and non-dialyzed. Secretomes were added to 250 mL flasks containing 1 g of autoclaved DMR-EH (120 °C, 20 min) in the presence of 10 mL sodium malonate (250 mM) at pH 7. Sterile distilled water was also added to achieve a total volume of 50 mL. Control treatments, without enzymes and with inactivated boiled secretome (utilizing the same volume of that treatment corresponding to the highest laccase dosage) were also carried out and analyzed at 1 and 4 days of incubation. Treatments were incubated at 30 °C and 150 rpm and samples collected after 1, 2, 3, and 4 days of treatment. At these time points, the flask contents were centrifuged at 5000 rpm for 20 min. The supernatant was collected and the solid fraction weighted after drying at 60 °C for 48 h. This solid fraction was then utilized for GPC analysis. All treatments were performed in duplicates.

DMR-EH treatment with the secretome of *P. eryngii* at pH7 in the presence and the absence of *P. putida* KT2440. The aim of this experiment was to evaluate if bacteria enhance lignin depolymerization in enzyme treatments with the *P. eryngii* secretome. For these experiments, the secretome was dialyzed in phosphate buffer (pH 7) as detailed previously and half of the volume boiled (20 min) to inactivate the enzymes. The treatments performed in this last experiment were (1) a control with DMR-EH and boiled secretome, (2) DMR-EH plus secretome (30 U laccase per g of DMR-EH), (3) DMR-EH plus boiled secretome and bacteria, and (4) DMR-EH plus secretome (30 U laccase per g DMR-EH) and bacteria. For these experiments, 1 g of DMR-EH was autoclaved (120 °C, 20 min) in the presence of 10 mL phosphate buffer (20 mM) at pH 7 in a 0.5 L beaker. Then, 10 mL of modified M9 media (×10), which is the growth media for the bacteria (pH 7), was also added and contained per L: 6.78 g Na_2HPO_4, 3 g KH_2PO_4, 0.5 g NaCl, and 15 mM $(NH_4)_2SO_4$. Then, 2 mL of 1 M $MgSO_4$, 100 μL of 1 M $CaCl_2$, and 1 mL of ion traces ($CuSO_4$, $MnSO_4$, $FeSO_4$, and $ZnSO_4$, 100 μM each) per L of treatment were added. The same phosphate buffer (20 mM) was finally added to achieve a total volume of 50 mL in all the treatments.

To grow and separate the bacteria, *P. putida* KT2440 (ATCC 47054), from the DMR-EH/enzyme mixture, a membrane system was employed. Dialysis membranes (cassettes) of 3.5 kDa cutoff (Thermo Scientific) were UV-sterilized for 20 minutes and inoculated with 2.5 mL of *P. putida* culture at an initial optical density (OD) of 0.1 at 600 nm. To prepare the bacterial inoculum, *P. putida* KT2440 was grown in LB at 30 °C and 220 rpm overnight. Cells were then centrifuged, washed, and diluted in modified M9 (×1) to reach the desired initial OD. Prior the experiments on lignin, the resistance of the cellulose-based dialysis membranes to the fungal secretome as well as the permeability of the membranes to LMW compounds was tested. For this purpose, inoculated membranes were incubated 3 days at 30 °C and 180 rpm in the presence of the secretome and only glucose (5 g L^{-1}) as carbon source in M9. For the experiments on lignin, inoculated membranes were then included in the corresponding beakers and treatments also incubated at 30 °C and 180 rpm during 3 days. Glucose was not added in these experiments. After the incubation, membranes were taken out and cells extracted with a syringe to quantify the final OD in a volume of 2.5 mL. The beaker contents were centrifuged at 5000 rpm for 20 minutes. Solids were dried for further weight, GPC, and compositional analysis. The supernatant was freeze-dried for GPC and LC-MS/MS analysis. All treatments were performed in duplicates.

Proteomic analysis in the secretome of *P. eryngii*

For proteomic analyses, 50 mL of the *P. eryngii* secretome from 9 days of incubation (used for the depolymerization assays) were taken from 2 biological replicates and flash-frozen. Then, samples were treated and analyzed as described in the ESI.† In brief, the volumes of the secretomes from *P. eryngii* were initially reduced prior to isolating the proteins with a chloroform–methanol extraction.[66] Then, the proteins were tryptically digested following a previously published protocol.[67] After this step, protein concentrations were normalized and

analyzed by LC-MS using a Velos Pro Orbitrap mass spectrometer (Thermo Scientific, San Jose, CA) outfitted with an electrospray ionization (ESI) interface coupled to custom built constant flow high-performance liquid chromatography (HPLC) system.[68,69] The MS/MS spectra from 15 LC-MS/MS datasets were converted to ASCII text (.dta format) using DeconMSn[70] and the data files were then interrogated *via* target-decoy approach[71] using MSGFPlus.[72] Protein sequences for each reported entry were subjected to BLAST analysis (version 2.2.28) using a combined collection of 2 784 909 fungal proteins reported in the Uniprot knowledgebase and NCBI. SignalP 4.0 [73] was finally utilized to predict the presence of signal peptide cleavage sites in the detected proteins.

Acknowledgements

We thank the US Department of Energy Bioenergy Technologies Office for funding this work. AP, MJM, and ATM acknowledge funding from INDOX (KBBE-2013-7-613549) EU project, RETO-PROSOT S2013/MAE-2907 Comunidad de Madrid BIO2015-68387-R MINECO, and NOESIS (BIO2014-56388-R) Spanish project. We thank Xiaowen Chen and Melvin Tucker for providing the DMR-EH substrate and Scott Baker for helpful discussions. The proteomics research was performed using EMSL, a DOE Office of Science User Facility sponsored by the Office of Biological and Environmental Research and located at Pacific Northwest National Laboratory. We also thank JGI-EMSL since a portion of this proteomic research was performed under the Facilities Integrating Collaborations for User Science (FICUS) initiative and used resources at the DOE Joint Genome Institute and the Environmental Molecular Sciences Laboratory, which are DOE Office of Science User Facilities. Both facilities are sponsored by the Office of Biological and Environmental Research and operated under Contract Nos. DE-AC02-05CH11231 (JGI) and DE-AC05-76RL01830 (EMSL). We thank our colleagues at Novozymes for providing Cellic CTec3 and HTec3.

Notes and references

1 A. T. Martínez, M. Speranza, F. Ruiz-Dueñas, P. Ferreira, S. Camarero, F. Guillén, M. J. Martínez, A. Gutiérrez and J. del Río, *Int. Microbiol.*, 2005, **8**, 195–204.
2 D. Salvachúa, A. Prieto, A. T. Martínez and M. J. Martínez, *Appl. Environ. Microbiol.*, 2013, **79**, 4316–4324.
3 P. Picart, P. D. de María and A. Schallmey, *Front Microbiol.*, 2015, **6**, 916.
4 T. D. Bugg, M. Ahmad, E. M. Hardiman and R. Rahmanpour, *Nat. Prod. Rep.*, 2011, **28**, 1883–1896.
5 T. Sonoki, Y. Iimura, E. Masai, S. Kajita and Y. Katayama, *J. Wood Sci.*, 2002, **48**, 429–433.
6 M. Ahmad, J. N. Roberts, E. M. Hardiman, R. Singh, L. D. Eltis and T. D. Bugg, *Biochemistry*, 2011, **50**, 5096–5107.
7 D. Salvachúa, E. M. Karp, C. T. Nimlos, D. R. Vardon and G. T. Beckham, *Green Chem.*, 2015, **17**, 4951–4967.
8 G. T. Beckham, C. W. Johnson, E. M. Karp, D. Salvachúa and D. R. Vardon, *Curr. Opin. Biotechnol.*, 2016, **42**, 40–53.
9 E. Fernández-Fueyo, F. J. Ruiz-Dueñas, M. F. López-Lucendo, M. Pérez-Boada, J. Rencoret, A. Gutiérrez, A. G. Pisabarro, L. Ramírez and A. T. Martínez, *Biotechnol. Biofuels*, 2016, **9**, 1–18.
10 D. Salvachúa, A. T. Martínez, M. Tien, M. Lopez-Lucendo, F. García, V. de los Ríos, M. J. Martínez and A. Prieto, *Biotechnol. Biofuels*, 2013, **6**, 115.
11 A. J. Ragauskas, G. T. Beckham, M. J. Biddy, R. Chandra, F. Chen, M. F. Davis, B. H. Davison, R. A. Dixon, P. Gilna, M. Keller, P. Langan, A. K. Naskar, J. N. Saddler, T. J. Tschaplinski, G. A. Tuskan and C. E. Wyman, *Science*, 2014, **344**, 1246843.
12 L. Munk, A. K. Sitarz, D. C. Kalyani, J. D. Mikkelsen and A. S. Meyer, *Biotechnol. Adv.*, 2015, **33**, 13–24.
13 A. Rico, J. Rencoret, J. del Río, A. T. Martínez and A. Gutiérrez, *Biotechnol. Biofuels*, 2014, **7**, 6.
14 C. Crestini, F. Melone and R. Saladino, *Bioorg. Med. Chem.*, 2011, **19**, 5071–5078.
15 H. Lange, S. Decina and C. Crestini, *Eur. Polym. J.*, 2013, **49**, 1151–1173.
16 D. Salvachúa, A. Prieto, M. L. Mattinen, T. Tamminen, T. Liitia, M. Lille, S. Willför, A. T. Martínez, M. J. Martínez and C. B. Faulds, *Enzyme Microb. Technol.*, 2013, **52**, 303–311.
17 S. Constant, H. L. J. Wienk, A. E. Frissen, P. d. Peinder, R. Boelens, D. S. van Es, R. J. H. Grisel, B. M. Weckhuysen, W. J. J. Huijgen, R. J. A. Gosselink and P. C. A. Bruijnincx, *Green Chem.*, 2016, **18**, 2651–2665.
18 M. R. Sturgeon, S. Kim, K. Lawrence, R. S. Paton, S. C. Chmely, M. Nimlos, T. D. Foust and G. T. Beckham, *ACS Sustainable Chem. Eng.*, 2014, **2**, 472–485.
19 S. Camarero, O. García, T. Vidal, J. Colom, J. del Río, A. Gutiérrez, J. Gras, R. Monje, M. J. Martínez and A. T. Martínez, *Enzyme Microb. Technol.*, 2004, **35**, 113–120.
20 S. Camarero, D. Ibarra, A. T. Martínez, J. Romero, A. Gutiérrez and J. del Río, *Enzyme Microb. Technol.*, 2007, **40**, 1264–1271.
21 D. Ibarra, M. Chavez, J. Rencoret, J. del Río, A. Gutiérrez, J. Romero, S. Camarero, M. J. Martínez, J. Jimenez-Barbero and A. T. Martínez, *Holzforschung*, 2007, **61**, 634–646.
22 E. Babot, A. Rico, J. Rencoret, L. Kalum, H. Lund, J. Romero, J. del Río, A. T. Martínez and A. Gutiérrez, *Bioresour. Technol.*, 2011, **102**, 6717–6722.

23 A. Gutiérrez, J. Rencoret, E. Cadena, A. Rico, D. Barth, J. del Río and A. T. Martínez, *Bioresour. Technol.*, 2012, **119**, 114–122.
24 M. Jurado, A. Prieto, A. Martínez-Alcalá, A. T. Martínez and M. J. Martínez, *Bioresour. Technol.*, 2009, **100**, 6378–6384.
25 J. Margot, C. Bennati-Granier, J. Maillard, P. Blanquez, D. A. Barry and C. Holliger, *AMB Express*, 2013, **3**, 63.
26 B. Viswanath, B. Rajesh, A. Janardhan, A. P. Kumar and G. Narasimha, *Enzyme Res.*, 2014, **2014**, 21.
27 J. G. Linger, D. R. Vardon, M. T. Guarnieri, E. M. Karp, G. B. Hunsinger, M. A. Franden, C. W. Johnson, G. Chupka, T. J. Strathmann, P. T. Pienkos and G. T. Beckham, *Proc. Natl. Acad. Sci. U. S. A.*, 2014, **111**, 12013–12018.
28 D. R. Vardon, M. A. Franden, C. W. Johnson, E. M. Karp, M. T. Guarnieri, J. G. Linger, M. J. Salm, T. J. Strathmann and G. T. Beckham, *Energy Environ. Sci.*, 2015, **8**, 617–628.
29 X. Chen, E. Kuhn, E. W. Jennings, R. Nelson, L. Tao, M. Zhang and M. P. Tucker, *Energy Environ. Sci.*, 2016, **9**, 1237–1245.
30 X. Chen, J. Shekiro, T. Pschorn, M. Sabourin, L. Tao, R. Elander, S. Park, E. Jennings, R. Nelson, O. Trass, K. Flanegan, W. Wang, M. E. Himmel, D. Johnson and M. P. Tucker, *Biotechnol. Biofuels*, 2014, **7**, 1–12.
31 L. Tao, X. Chen, A. Aden, E. Kuhn, M. E. Himmel, M. Tucker, M. A. A. Franden, M. Zhang, D. K. Johnson and N. Dowe, *Biotechnol. Biofuels*, 2012, **5**, 1.
32 S. D. Mansfield, H. Kim, F. Lu and J. Ralph, *Nat. Protoc.*, 2012, **7**, 1579–1589.
33 K. Hoon, J. Ralph and T. Akiyama, *BioEnergy Res.*, 2008, **1**, 56–66.
34 J. J. Bozell, C. J. O'Lenick and S. Warwick, *J. Agric. Food Chem.*, 2011, **59**, 9232–9242.
35 S. Fornale, J. Rencoret, L. García-Calvo, M. Capellades, A. Encina, R. Santiago, J. Rigau, A. Gutiérrez, J. C. Del Río and D. Caparrós-Ruiz, *Plant Sci.*, 2015, **236**, 272–282.
36 D. Linde, F. J. Ruiz-Dueñas, E. Fernández-Fueyo, V. Guallar, K. E. Hammel, R. Pogni and A. T. Martínez, *Arch. Biochem. Biophys.*, 2015, **574**, 66–74.
37 E. Fernández-Fueyo, F. J. Ruiz-Dueñas, M. J. Martínez, A. Romero, K. E. Hammel, F. J. Medrano and A. T. Martínez, *Biotechnol. Biofuels*, 2014, **7**, 2–2.
38 A. T. Martínez, *Enzyme Microb. Technol.*, 2002, **30**, 425–444.
39 S. F. Altschul, W. Gish, W. Miller, E. W. Myers and D. J. Lipman, *J. Mol. Biol.*, 1990, **215**, 403–410.
40 C. M. Payne, B. C. Knott, H. B. Mayes, H. Hansson, M. E. Himmel, M. Sandgren, J. Ståhlberg and G. T. Beckham, *Chem. Rev.*, 2015, **115**, 1308–1448.
41 D. Salvachúa, A. Prieto, M. Lopez-Abelairas, T. Lu-Chau, A. T. Martínez and M. J. Martínez, *Bioresour. Technol.*, 2011, **102**, 7500–7506.
42 C. Zhao, S. Xie, Y. Pu, R. Zhang, F. Huang, A. J. Ragauskas and J. S. Yuan, *Green Chem.*, 2016, **18**, 1306–1312.
43 T. D. Bugg, M. Ahmad, E. M. Hardiman and R. Singh, *Curr. Opin. Biotechnol.*, 2011, **22**, 394–400.
44 D. Salvachúa, A. Prieto, M. Vaquero, A. T. Martínez and M. J. Martínez, *Bioresour. Technol.*, 2013, **131**, 218–225.
45 C. Muñoz, F. Guillén, A. T. Martínez and M. J. Martínez, *Appl. Environ. Microbiol.*, 1997, **63**, 2166–2174.
46 A. Heinfling, M. J. Martínez, A. T. Martínez, M. Bergbauer and U. Szewzyk, *FEMS Microbiol. Lett.*, 1998, **165**, 43–50.
47 J. Ramos, T. Rojas, F. Navarro, F. Davalos, R. Sanjuan, J. Rutiaga and R. A. Young, *J. Agric. Food Chem.*, 2004, **52**, 5057–5062.
48 S. Camarero, D. Ibarra, Á. T. Martínez, J. Romero, A. Gutiérrez and J. C. del Río, *Enzyme Microb. Technol.*, 2007, **40**, 1264–1271.
49 S. Camarero, A. I. Cañas, P. Nousiainen, E. Record, A. Lomascolo, M. J. Martínez and Á. T. Martínez, *Environ. Sci. Technol.*, 2008, **42**, 6703–6709.
50 A. I. Cañas and S. Camarero, *Biotechnol. Adv.*, 2010, **28**, 694–705.
51 J. S. Dordick, M. A. Marletta and A. M. Klibanov, *Proc. Natl. Acad. Sci. U. S. A.*, 1986, **83**, 6255–6257.
52 D. N. Thompson, B. R. Hames, C. A. Reddy and H. E. Grethlein, *Biotechnol. Bioeng.*, 1998, **57**, 704–717.
53 V. Sáez-Jiménez, M. C. Baratto, R. Pogni, J. Rencoret, A. Gutiérrez, J. I. Santos, A. T. Martínez and F. J. Ruiz-Dueñas, *J. Biol. Chem.*, 2015, **290**, 23201–23213.
54 Q. Chen, M. Marshall, S. Geib, M. Tien and T. Richard, *Bioresour. Technol.*, 2012, **117**, 186–192.
55 R. Martin-Sampedro, E. A. Capanema, I. Hoeger, J. C. Villar and O. J. Rojas, *J. Agric. Food Chem.*, 2011, **59**, 8761–8769.
56 R. Bourbonnais, M. G. Paice, I. D. Reid, P. Lanthier and M. Yaguchi, *Appl. Environ. Microbiol.*, 1995, **61**, 1876–1880.
57 M. Hofrichter, T. Lundell and A. Hatakka, *Appl. Environ. Microbiol.*, 2001, **67**, 4588–4593.
58 S. Gronqvist, L. Viikari, M. L. Niku-Paavola, M. Orlandi, C. Canevali and J. Buchert, *Appl. Microbiol. Biotechnol.*, 2005, **67**, 489–494.
59 J. R. Hernández Fernaud, A. Carnicero, F. Perestelo, M. Hernández Cutuli, E. Arias and M. A. Falcón, *Enzyme Microbiol. Technol.*, 2006, **38**, 40–48.
60 L. Marzullo, R. Cannio, P. Giardina, M. T. Santini and G. Sannia, *J. Biol. Chem.*, 1995, **270**, 3823–3827.
61 H. W. Kern and T. K. Kirk, *Appl. Environ. Microbiol.*, 1987, **53**, 2242–2246.
62 A. Hernández-Ortega, P. Ferreira and A. T. Martínez, *Appl. Microbiol. Biotechnol.*, 2012, **93**, 1395–1410.
63 X. Chen, J. Shekiro, R. Elander and M. Tucker, *Ind. Eng. Chem. Res.*, 2012, **51**, 70–76.
64 A. Sluiter, B. Hames, R. Ruiz, C. Scarlata, J. Sluiter and D. Templeton, *Determination of sugars, byproducts, and degradation products in liquid fraction process samples*, NREL Laboratory Analytical Procedure, 2006.
65 M. G. Resch, J. O. Baker and S. R. Decker, *Low solids enzymatic saccharification of lignocellulosic biomass*, NREL Laboratory Analytical Procedure, 2015.

66 D. Wessel and U. I. Flügge, *Anal. Biochem.*, 1984, **138**, 141–143.
67 S. J. Callister, M. A. Domínguez, C. D. Nicora, X. Zeng, C. L. Tavano, S. Kaplan, T. J. Donohue, R. D. Smith and M. S. Lipton, *J. Proteome Res.*, 2006, **5**, 1940–1947.
68 A. Maiolica, D. Borsotti and J. Rappsilber, *Proteomics*, 2005, **5**, 3847–3850.
69 R. T. Kelly, J. S. Page, Q. Luo, R. J. Moore, D. J. Orton, K. Tang and R. D. Smith, *Anal. Chem.*, 2006, **78**, 7796–7801.
70 A. M. Mayampurath, N. Jaitly, S. O. Purvine, M. E. Monroe, K. J. Auberry, J. N. Adkins and R. D. Smith, *Bioinformatics*, 2008, **24**, 1021–1023.
71 J. E. Elias and S. P. Gygi, in *Proteome Bioinformatics*, ed. J. S. Hubbard and R. A. Jones, Humana Press, Totowa, NJ, 2010, pp. 55–71, DOI: 10.1007/978-1-60761-444-9_5.
72 S. Kim and P. A. Pevzner, *Nat. Commun.*, 2014, 5.
73 T. N. Petersen, S. Brunak, G. von Heijne and H. Nielsen, *Nat. Methods*, 2011, **8**, 785–786.

Electronic Supplementary Information for:

Lignin depolymerization by fungal secretomes and a microbial sink†

Davinia Salvachúa[a,‡], Rui Katahira[a,‡], Nicholas S. Cleveland[a], Payal Khanna[a], Michael G. Resch[a], Brenna A. Black[a], Samuel O. Purvine[b], Erika M. Zink[b], Alicia Prieto[c], María J. Martínez[c], Angel T. Martínez[c], Blake A. Simmons[d,e], John M. Gladden[d,f], Gregg T. Beckham[a,*]

a. National Bioenergy Center, National Renewable Energy Laboratory (NREL), Golden CO 80401, USA
b. Environmental Molecular Sciences Laboratory, Pacific Northwest National Laboratory (PNNL), Richland, WA 99352, USA
c. Centro de Investigaciones Biológicas, Consejo Superior de Investigaciones Científicas (CSIC), E-28040 Madrid, Spain
d. Joint BioEnergy Institute (JBEI), Emeryville, CA 94608
e. Biological Systems and Engineering, Lawrence Berkeley National Laboratory, Berkeley CA 94720 USA
f. Sandia National Laboratory, Livermore CA 94550
‡ Equal contribution
* Corresponding author: Gregg.Beckham@nrel.gov

Extension of materials and methods section

Analysis of aromatics by LC-MS/MS

Mass spectrometry was used in the last experiment of the current study to analyze aromatics from the soluble fraction. For this purpose, 14.5 mg of freeze-dried supernatant from 8 different treatments was reconstituted in 1 mL methanol. Analysis of samples was performed on an Agilent 1100 LC system equipped with a diode array detector (DAD) and an Ion Trap SL MS (Agilent Technologies, Palo Alto, CA) with in-line electrospray ionization (ESI). Each sample was injected at a volume of 25 µL into the LC-MS system. Primary degradation compounds were separated using a YMC C30 Carotenoid 0.3 µm, 4.6 x 150 mm column (YMC America, Allentown, PA) at an oven temperature of 30°C. The HPLC solvent gradient was performed using eluents of A) water modified with ammonium hydroxide (pH 7), and eluent B) 9:1 acetonitrile and water also modified with ammonium hydroxide (pH 7). At a flow rate of 0.7 mL min^{-1}, the gradient chromatography was as follows: 0-3 min, 0% B; at 16 min, 7% B; at 21 min, 8.5% B; at 34 min, 10% B; at 46 min, 25% B; and held at 30% B at 51-56 min, for a total run time of 65 min including equilibrium. Flow from the HPLC-DAD was directly routed to the ESI/MS ion trap. The DAD was used to monitor chromatography at 210 nm for a direct comparison to MS data. MS and MS/MS tuned parameters are as follows: smart parameter setting with target mass set to 165 Da, compound stability 70%, trap drive 50%, capillary at 3500 V, fragmentation amplitude of 0.75 V with a 30 to 200% ramped voltage implemented for 50 msec, and an isolation width of 2 m/z (He collision gas). The ESI nebulizer gas was set to 60 psi, with dry gas flow of 11 L min^{-1} held at 350°C. MS scans and precursor isolation-fragmentation scans were performed across the range of 40-350 Da in negative- and positive-ion alternating mode. Vanillin, 4-hydroxybenzaldehyde, PCA, vanillic acid, syringic acid, 4-hydroxybenzoic acid, and FA were the only aromatics detected from an instrument specific in-house database of 70 aromatic compounds. Standards were prepared in the range of 1 – 100 µg/mL and run at the same conditions as the samples. Samples were diluted accordingly to maintain detector response within the linear range of the calibration curves (R^2 value of ≥99.5%).

Proteomic analysis in the secretome of P. eryngii

For proteomic analyses, 50 mL of the *P. eryngii* secretome from 9 days of incubation (used for the depolymerization assays) were taken from 2 biological replicates and flash-frozen. Then, samples were treated and analyzed as described below:

Volume concentration. The volumes of the secretomes from *P. eryngii* were initially reduced prior to isolating the proteins with a chloroform-methanol extraction. To reduce the volumes, centrifugal filters (MilliporeAmicon Ultra-15, 10k MWCO) were used following the vendor protocol for volume concentration. Briefly, the proteins were first denatured by adding 8 M urea and incubating for 1 h at 37°C. The denatured proteins were then added to a spin filter that had been pre-rinsed with 0.1 N NaOH and then 50 mM NH_4HCO_3. The sample was then added to the spin filter and concentrated to less than 0.5 mL by centrifugation (3220 x g, 2 h) at room temperature. The concentrated sample was rinsed three times with 8 M urea in 50 mM NH_4HCO_3 before transferring to a 15-mL Falcon tube that was methanol-chloroform compatible. The volumes were normalized and then the samples were flash frozen and stored at -70°C until ready for extraction.

Methanol-chloroform extraction. Any residual detergents or lipids were removed by performing a methanol-chloroform extraction.[1] Keeping each sample on ice, based on the sample volume (Svol), 4x the Svol of chilled methanol (-20°C) and 1x the Svol of chilled chloroform (-20°C) was added. The samples were vortexed gently before adding 3x Svol of chilled nanopure water (4°C) and vortexed to mix well before chilling on ice for 5 minutes. The layers were separated using centrifugation (8k x g, 4°C, 15 minutes) and the top layer was carefully removed and discarded. An additional 3x Svol was added to the tube, the sample was vortexed to mix well, and the proteins were isolated by centrifugation (8k x g, 4°C, 15 minutes) and removal of the supernatant. The protein pellet was allowed to dry completely under nitrogen before resuspending into 8 M urea in 50 mM NH_4HCO_3 and immediately digested.

Tryptic Digestion. The proteins were tryptically digested following a previously published protocol[2] with the following modifications. The proteins were first denatured with 5 mM dithiotreitol for 30 minutes at 60°C in a thermomixer. After cooling for a few minutes, the samples were diluted 10-fold with 50 mM NH_4HCO_3 and 1 mM $CaCl_2$ was added. A trypsin solution (1 µg/uL in 5 mM acetic acid, UBX) was added at an enzyme-to-protein ratio of 1:50 and the samples were incubated for 3 h at 37°C in a thermomixer. The digested proteins were desalted using a C18 SPE column (Supelco) and the final protein concentration was estimated using a BCA protein assay (Pierce). The concentrations were normalized and a portion was diluted to 0.1 ug/uL to be analyzed by LC-MS.

LC-MS Analysis. Data were acquired using a Velos Pro Orbitrap mass spectrometer (Thermo Scientific, San Jose, CA) outfitted with an electrospray ionization (ESI) interface coupled to custom built constant flow high-performance liquid chromatography (HPLC) system. The LC system consisted of two Agilent 1200 nanoflow pumps (Agilent Technologies, Santa Clara, CA), various Valco valves (Valco Instruments Co., Houston, TX), and a PAL autosampler (Leap Technologies, Carrboro, NC). Software developed in-house allowed for automated event coordination of two parallel reversed-phase analytical columns prepared in-house by slurry packing 3-µm Jupiter C18 (Phenomenex, Torrence, CA) into 40-cm x 360 µm o.d. x 75 µm i.d fused silica (Polymicro Technologies Inc., Phoenix, AZ) using a 1-cm sol-gel frit for media retention.[3] Electrospray emitters were custom made using 150 um o.d. x 20 um i.d. chemically etched fused silica.[4] Mobile phases consisted of 0.1% formic acid in water (A) and 0.1% formic acid acetonitrile (B) with a gradient profile as follows (min:%B); 0:5, 2:8, 20:12, 75:35, 97:60, 100: 85 at a flow rate of 300 nL/min. The gradient start was triggered 20 minutes after injecting a 5 uL sample aliquot with data acquisition beginning 15 minutes into the gradient to account for column dead volume. Ion transfer tube temperature and spray voltage were 350°C and 2.2 kV, respectively. Orbitrap spectra (AGC 1x106) were collected for 100 minutes over the mass (m/z) range of 400-2000 at a resolution of 60K followed by data dependent ion trap CID MS/MS (AGC 3x104) of the 10 most abundant ions using a collision energy of 35% and activation time 10 ms. A dynamic exclusion time of 60 seconds was used to discriminate against previously analyzed ions. The parallel use of two columns, allowed each column to be re-generated off-line at the end of each run.

Data search and protein identification. The MS/MS spectra from 15 LC-MS/MS datasets were converted to ASCII text (.dta format) using DeconMSn[5] which attempts to more precisely assign the charge and parent mass values to an MS/MS spectrum. The data files were then interrogated via target-decoy approach[6] using MSGFPlus[7] using a +/- 20 ppm parent mass tolerance, partially tryptic enzyme settings (one end of each candidate sequence must contain Lysine or Arginine), and a variable posttranslational modification of oxidized Methionine. All MS/MS search results for each dataset were collated into tab separated ASCII text.

Collated search results were further combined into a single result file. These results were imported into a Microsoft SQL Server database. Using decoy identifications (exactly reversed peptide sequences denoted as "XXX_" in their protein references), we determined the PSM level FDR to be less than 1% when using MSGFPlus's Q-value calculation (681 reversed PSMs from a total 71,995 filter passing PSMs using Q-value <= 0.01). Filter passing results were reported in Table S1. Using the protein references as a grouping term, unique peptides belonging to each protein were counted, as were all PSMs belonging to all peptides for that protein (i.e. a protein level observation count value). PSM observation counts were summed across biological replicates, and were also reported in the excel file. Using the pivot function in excel, a cross-tabulation table was created to enumerate protein level PSM observations for each of the five combined replicate samples, allowing low-precision quantitative comparisons to be made between each sample at the protein level.

Protein sequences for each reported entry were subjected to BLAST analysis (version 2.2.28) using a combined collection of 2,784,909 fungal proteins reported in the Uniprot knowledgebase and NCBI as of September 2014. Results were imported into SQL Server and the highest-similarity identification (lowest e-value, highest percent similarity) extracted. As many of these matches resulted in an uncharacterized or hypothetical protein reference, the highest similarity non-hypothetical entry (does NOT contain "Uncharacterized", "predicted protein", "hypothetical", or "Unplaced") was also extracted for each query allowing for more useful biological inferences to be made. All BLAST results were imported into the excel file and related to the cross-tabulated results to allow further investigation. SignalP 4.0[8] was finally utilized to predict the presence of signal peptide cleavage sites in the detected proteins.

References

1. D. Wessel and U. I. Flugge, *Anal. Bioochem.*, 1984, 138, 141-143.
2. S. J. Callister, M. A. Domínguez, C. D. Nicora, X. Zeng, C. L. Tavano, S. Kaplan, T. J. Donohue, R. D. Smith and M. S. Lipton, *J. Proteome Res.*, 2006, 5, 1940-1947.
3. A. Maiolica, D. Borsotti and J. Rappsilber, *Proteomics*, 2005, 5, 3847-3850.
4. R. T. Kelly, J. S. Page, Q. Luo, R. J. Moore, D. J. Orton, K. Tang and R. D. Smith, *Anal. Chem.*, 2006, 78, 7796-7801.
5. A. M. Mayampurath, N. Jaitly, S. O. Purvine, M. E. Monroe, K. J. Auberry, J. N. Adkins and R. D. Smith, *Bioinformatics*, 2008, 24, 1021-1023.
6. J. E. Elias and S. P. Gygi, in *Proteome Bioinformatics*, eds. J. S. Hubbard and R. A. Jones, Humana Press, Totowa, NJ, 2010, DOI: 10.1007/978-1-60761-444-9_5, 55-71.
7. S. Kim and P. A. Pevzner, *Nat. Commun.*, 2014, 5.
8. T. N. Petersen, S. Brunak, G. von Heijne and H. Nielsen, *Nat. Meth.*, 2011, 8, 785-786.

Figures

Fig. S1: Detection of oxidoreductases in the secretome of twelve white-rot fungi: (A) Laccase activity tracked by the oxidation of 5 mM 2,2´-azino-bis(3-ethylbenzthiazoline-6-sulfonic acid) (ABTS) at pH 5 and (B) peroxidase (e.g. manganese peroxidase (MnP) and versatile peroxidase (VP)) activity tracked by the oxidation of 0.1 mM $MnSO_4$ in the presence of 0.1 mM H_2O_2 at pH5. Data are the result of biological duplicates. The fungi presented in the manuscript are denoted in bold.

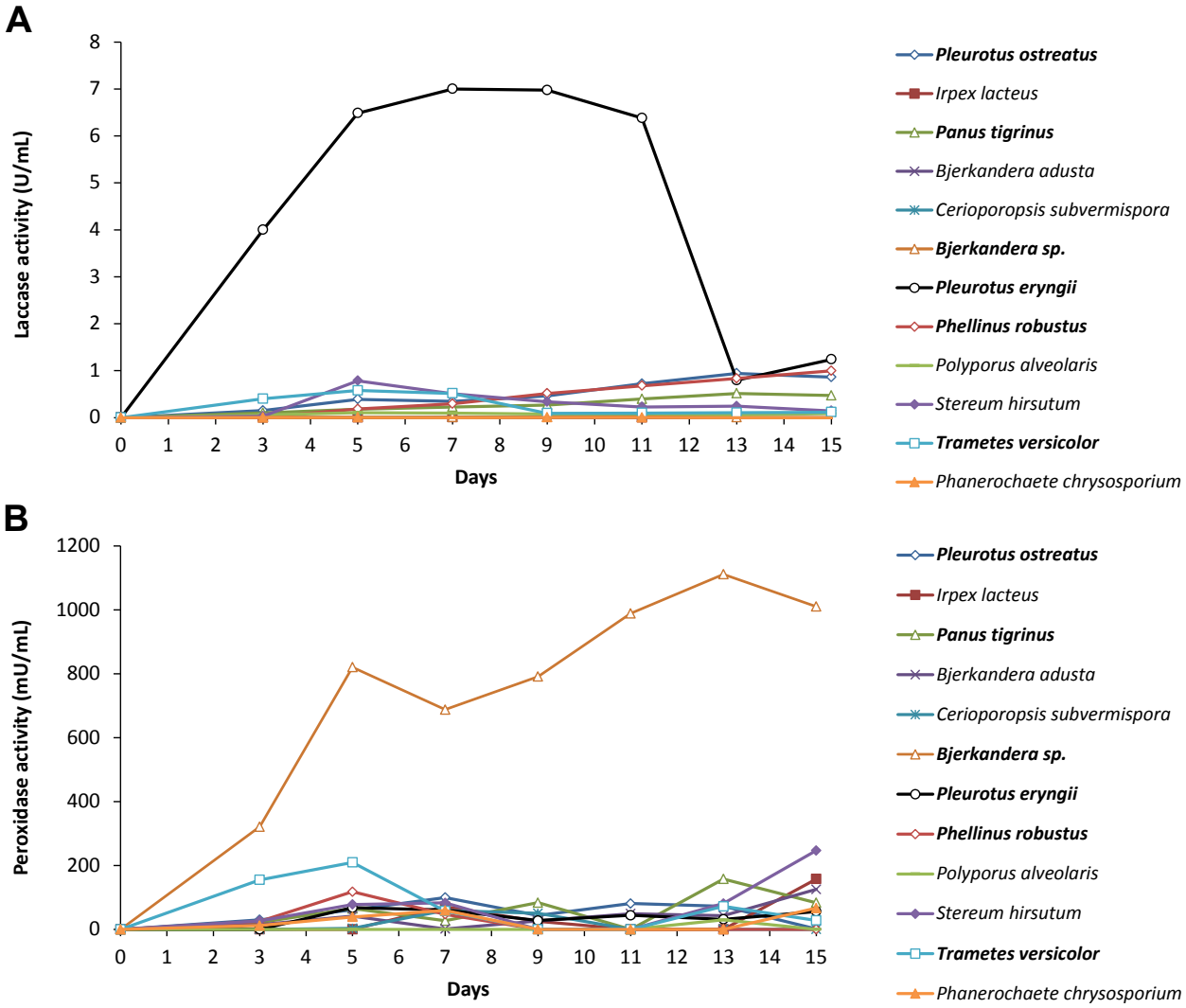

Tables:

Table S1: GPC results (M_p, M_n, M_w, PD) - associated to Fig. 4 in the main manuscript- from DMR-EH lignin before and after the enzyme treatments with the fungal secretomes at 3 and 6 days . Tables show the results from treatments with the *P. eryngii* secretome at **(A)** pH 4.5 and **(B)** pH 7, treatments with **(C)** *Bjerkandera* sp. secretome at pH 4.5 and treatments with **(D)** both fungal secretomes at pH 4.5. Enzyme treatments on DMR-EH lignin were conducted over 3 and 6 days at 30°C and 150 rpm. H_2O_2 and Mn^{2+} were added periodically to treatments containing peroxidases and to the corresponding controls (CTL). Enzyme dosages are expressed as U of

enzyme per gram of DMR-EH lignin. Laccase (LA) and peroxidase (PE) activities were calculated following the oxidation of ABTS at the corresponding pH in the absence or the presence of Mn^{2+} and H_2O_2, respectively. The asterisk (*) highlights 3-day treatments.

***(A) P. eryngii* secretome pH 4.5**

	Day	M_p	M_n	M_w	PD
CTL	**6**	4100	1900	12000	6.7
10 U/g	**6**	4100	1700	9600	5.7
50 U/g	**6**	3900	1500	7700	5.2
100 U/g	**6**	3600	1100	5600	4.9
100 U/g*	**3**	3600	1200	5400	4.6

***(B) P. eryngii* secretome pH 7**

	Day	M_p	M_n	M_w	PD
CTL	**6**	3700	1300	6100	4.5
3 U/g	**6**	3800	1400	7400	5.3
15 U/g	**6**	3700	1500	5600	3.8
30 U/g	**6**	3200	840	3200	3.8
30 U/g*	**3**	390	530	2300	4.4

***(C) Bjerkandera* sp. secretome pH 4.5**

	Day	M_p	M_n	M_w	PD
CTL	**6**	4100	1800	12000	6.5
8 U/g	**6**	4100	2100	15000	7.1
40 U/g	**6**	3900	1900	11000	5.7
80 U/g	**6**	3500	950	5600	5.8
80 U/g*	**3**	4100	1700	11000	6.3

(I

	Day	M_p	M_n	M_w	PD
CTL	**6**	4100	1800	12000	6.5
5 U/g LA + 4 U/g PE	**6**	3900	1300	10000	7.9
25 U/g LA + 20 U/g PE	**6**	4100	1500	8800	6.0
50 U/g LA + 40 U/g PE	**6**	3400	620	3500	5.6
50 U/g LA + 40 U/g PE*	**3**	390	700	2000	2.9

Table S2: GPC results (M_p, M_n, M_w, PD) - associated to Fig. 4D in the main manuscript- as a function of time from *P. eryngii* secretome treatments at pH 7 over 4 days of incubation. DMR-EH lignin M_p, M_n, and PD by using different laccase dosages (3, 10, 30 U/g LA) from non-dialyzed secretomes. The asterisk (*) at 4 days corresponds to the control that contains boiled secretome.

Control	M_p	M_n	PD
1 d	3450 ± 50	1850 ± 150	3.2 ± 0.0
4 d	3400 ± 0	1800 ± 0	2.9 ± 0.2
4 d*	3450 ± 50	1850 ± 150	3.1 ± 0.0

3 U/g LA	M_p	M_n	PD
1 d	3550 ± 50	1300 ± 0	4.1 ± 0.0
2 d	3600 ± 0	1300 ± 0	4.0 ± 0.3
3 d	3350 ± 50	1250 ± 50	3.5 ± 0.2
4 d	3650 ± 50	1850 ± 50	3.0 ± 0.1

10 U/g LA	M_p	M_n	PD
1 d	3500 ± 100	1300 ± 0	4.2 ± 0.6
2 d	3400 ± 0	1250 ± 50	3.7 ± 0.0
3 d	3300 ± 0	1050 ± 50	3.4 ± 0.2
4 d	3500 ± 0	1500 ± 100	3.1 ± 0.1

30 U/g LA	M_p	M_n	PD
1 d	3350 ± 50	900 ± 100	3.8 ± 0.4
2 d	3250 ± 50	950 ± 50	4.6 ± 1.0
3 d	3200 ± 0	800 ± 0	3.8 ± 0.2
4 d	3350 ± 50	1150 ± 50	3.8 ± 0.1

Table S3: Incubation of DMR-EH lignin, the *P. eryngii* secretome, and *P. putida* KT2440 to demonstrate the microbial sink concept. (A) DMR-EH with fungal secretome and bacteria. **(B)** Bacterial growth after the treatment represented in (B). **(C)** DMR-EH lignin M_w obtained from the different treatments in the insoluble and soluble fractions. **(D)** GPC profiles of DMR-EH lignin and other GPC parameters from the insoluble fraction after the different treatments. **(E)** LC-MS/MS from the soluble fraction at the end point of the different treatments. DMR = DMR-EH with inactivated fungal secretome; DMR+S = DMR-EH with fungal secretome; DMR + B = DMR-EH with bacteria and inactivated secretome; DMR + S + B = DMR-EH with bacteria and fungal secretome; 4-HBA: 4-hydroxybenzoic acid; 4-HB: 4-hydroxybenzaldehyde.

	M_p	M_n	PD
DMR	3550 ± 50	1650 ± 50	5.0 ± 0.2
DMR + B	3567 ± 58	1633 ± 58	4.5 ± 0.1
DMR + S	3350 ± 50	1200 ± 100	4.3 ± 0.2
DMR + B + S	3100 ± 100	920 ± 10	4.0 ± 0.3

Table S4: Proteomic analysis of the secretome of *Pleurotus eryngii* after 9 days of incubation in the presence of DMR-EH lignin. Protein descriptions are based on the most similar fungal proteins found in Uniprot/NCBI databases (whose access numbers and fungal species are indicated) and organized by functional families: (A) oxidoreductases, (B) glycoside hydrolases, (C) proteinases, (D) esterases, (E) proteins with another function, and (F) proteins with unknown function. The analysis is the result of biological duplicates. E-values, identity, and the presence or absence of a signal peptide (predicted by SignalP) from the different proteins are also included. Proteins in each functional group are organized by "spectral mass counts number" in order of abundance.

(A) OXIDOREDUCTASES							
Best BLAST non-hypothetical					**Spectral mass counts**		**Signal peptide**
Access number	**Protein description**	**Fungi**	**E-value**	**Identity (%)**	**Average**	**Error**	
A0A0D2N8Y9_9AGAR	GMC oxidoreductase	*Hypholoma sublateritium*	0	53.06	**1890**	103	YES
Q96TR4_PLEOS	Laccase	*Pleurotus ostreatus*	0	98.08	**700**	69	YES
D3YBH4_PLEER	Aryl-alcohol oxidase	*Pleurotus eryngii*	0	99.16	**664**	1	YES
A0A0C2Y131_HEBCY	Copper radical oxidase	*Hebeloma cylindrosporum*	0	76.96	**275**	4	YES
Q9UVY4_PLEOS	Bilirubin oxidase	*Pleurotus ostreatus*	0	98.12	**268**	45	YES
A0A0D2N8Y9_9AGAR	GMC oxidoreductase	*Hypholoma sublateritium*	0	53.06	**259**	11	YES
B6V331_PLEER	Laccase	*Pleurotus eryngii*	0	100	**239**	2	YES
V2WWR3_MONRO	Putative FAD dependent oxidoreductase	*Moniliophthora roreri*	0	64.35	**206**	13	YES
A0AQZ6_PLEOS	POXA3b laccase small subunit	*Pleurotus ostreatus*	2E-124	97.31	**205**	15	YES
A0A067NSZ9_PLEOS	Laccase	*Pleurotus ostreatus*	0	94.55	**155**	1	YES
A0A067N4E7_PLEOS	DyP-type peroxidase	*Pleurotus ostreatus*	0	91.87	**118**	10	NO
A0A067PAG4_PLEOS	Putative GMC-oxidase	*Pleurotus ostreatus*	0	95.15	**113**	12	YES
A0A067NHL8_PLEOS	DyP-type peroxidase	*Pleurotus ostreatus*	0	97.48	**105**	7	YES
Q9P928_PLEPU	Aryl-alcohol oxidase	*Pleurotus pulmonaris*	0	50.17	**59**	5	YES
O94219_PLEER	Aryl-alcohol oxidase	*Pleurotus eryngii*	0	57.82	**50**	4	YES
V2XEX2_MONRO	Copper radical oxidase	*Moniliophthora roreri*	0	60.07	**44**	6	YES
gi|636619781|ref|XP_008041025.1|	Aldo/keto reductase	*Trametes versicolor*	3E-149	68.32	**43**	9	NO
M5BNG8_THACB	Glucose oxidase	*Thanatephorus cucumeris*	8E-173	46.31	**39**	1	YES
A0A0D2N8Y9_9AGAR	GMC oxidoreductase	*Hypholoma sublateritium*	0	53.06	**39**	4	YES
A0A0C3DRC3_9HOMO	Glyoxal oxidase	*Moniliophthora roreri*	0	72.33	**33**	1	YES
A0A0H2RBF2_9HOMO	Alcohol oxidase	*Schizopora paradoxa*	0	55.94	**28**	1	YES
A0A067NPB6_PLEOS	Multi-copper oxidase superfamily	*Pleurotus ostreatus*	0	95.01	**20**	4	YES
V2X5U0_MONRO	Tyrosinase central domain-containing protein	*Moniliophthora roreri*	2E-135	56.25	**18**	1	YES
B0DZR8_LACBS	Glyoxal oxidase	*Laccaria bicolor*	0	73.33	**16**	1	YES
A0A0C3DRC3_9HOMO	Glyoxal oxidase	*Rhizoctonia solani*	0	72.33	**14**	2	YES
gi|636608221|ref|XP_008035245.1|	Glyoxal oxidase precursor	*Trametes versicolor*	0	79.51	**14**	2	NO
V2X162_MONRO	Aryl-alcohol oxidase	*Moniliophthora roreri*	0	52.9	**11**	2	YES
gi|636621931|ref|XP_008042100.1|	Glyoxal oxidase precursor	*Trametes versicolor*	0	75.8	**9**	0	YES
gi|597979803|ref|XP_007363089.1|	GMC oxidoreductase	*Dichomitus squalens*	0	56.44	**7**	1	YES
gi|636621933|ref|XP_008042101.1|	FMN-linked oxidoreductase	*Trametes versicolor*	0	68.46	**7**	1	NO
V2WN23_MONRO	Aryl-alcohol oxidase	*Moniliophthora roreri*	1E-129	49.29	**6**	1	NO
D3YJ58_PLEER	Laccase	*Pleurotus eryngii*	0	99.81	**5**	1	YES
A0A0D7B374_9HOMO	FMN-linked oxidoreductase	*Cylindrobasidium torrendii*	2E-163	61.39	**5**	1	NO
A0A067NL45_PLEOS	Small subunit of laccase POXA3a	*Pleurotus ostreatus*	4E-118	94.57	**5**	2	YES

B5MAF4_PLEOS	Phenol oxidase	*Pleurotus ostreatus*	0	97.89	**5**	2	YES
A0A0D2N8Y9_9AGAR	GMC oxidoreductase	*Hypholoma sublateritium*	0	53.06	**4**	1	YES
A0A0D2N8Y9_9AGAR	GMC oxidoreductase	*Hypholoma sublateritium*	0	53.06	**3**	1	YES
A0A0D2KZY8_9AGAR	Copper radical oxidase	*Hypholoma sublateritium*	0	69.24	**3**	1	YES
A0A0D7B374_9HOMO	FMN-linked oxidoreductase	*Cylindrobasidium torrendii*	2E-163	61.39	**3**	1	NO
gi|597979803|ref|XP_007363089.1|	GMC oxidoreductase	*Dichomitus squalens*	0	56.44	**3**	1	YES
V2WIU4_MONRO	Glutathione-disulfide reductase	*Moniliophthora roreri*	0	77.22	**2**	1	NO
A0A067NUD9_PLEOS	Multi-copper oxidase	*Pleurotus ostreatus*	0	94.8	**2**	1	YES

(B) GLYCOSIDE HYDROLASES							
Best BLAST non-hypothetical			**E-value**	**Identity (%)**	**Spectral mass counts**		**Signal peptide**
Access number	**Protein description**	**Fungi**			**Average**	**Error**	
S7QEU8_GLOTA	Cerato-platanin	*Gloeophyllum trabeum*	3E-61	66.2	**971**	78	YES
gi|636609529|ref|XP_008035899.1|	Cerato-platanin	*Trametes versicolor*	2E-66	71.43	**519**	37	YES
G0TES6_PLEOS	Alfa-L-arabinofuranosidase	*Pleurotus ostreatus*	0	96.13	**195**	33	YES
A0A067NJI9_PLEOS	Glucoamylase	*Pleurotus ostreatus*	0	96.2	**140**	24	YES
A0A067NAN6_PLEOS	Glycoside hydrolase family 79 protein	*Pleurotus ostreatus*	0	97.25	**135**	9	YES
A0A067NTS1_PLEOS	1,3-beta-glucanosyltransferase	*Pleurotus ostreatus*	0	98.41	**126**	4	YES
A0A067P251_PLEOS	Glycoside hydrolase family 3 protein	*Pleurotus ostreatus*	0	95.88	**75**	12	YES
A0A067NVM1_PLEOS	alpha-1,2-Mannosidase	*Pleurotus ostreatus*	0	97.41	**68**	16	YES
A0A067NV32_PLEOS	Carbohydrate-binding module family 13 protein	*Pleurotus ostreatus*	0	93.7	**60**	8	NO
A0A067NE06_PLEOS	Glycoside hydrolase family 32 protein	*Pleurotus ostreatus*	0	93.05	**60**	4	YES
A0A0D7BL56_9HOMO	Glycoside hydrolase family 30 protein	*Rhizoctonia solani*	0	61.39	**60**	8	YES
S3DB13_GLAL2	Six-hairpin glycosidase	*Glarea lozoyensis*	2E-164	40.32	**57**	27	YES
A0A067NYS5_PLEOS	Glycoside hydrolase family 79 protein	*Pleurotus ostreatus*	0	95.39	**56**	3	YES
A0A067P1A5_PLEOS	Glycoside hydrolase family 3 protein	*Pleurotus ostreatus*	0	96.21	**50**	0	YES
A0A067NNN7_PLEOS	Glycoside hydrolase family 43 protein	*Pleurotus ostreatus*	0	88.99	**49**	1	YES
A0A074RMJ0_9HOMO	Putative glycoside hydrolase family 43 protein	*Rhizoctonia solani*	0	61.28	**47**	8	YES
A0A067N9V0_PLEOS	Glycoside hydrolase family 3 protein	*Pleurotus ostreatus*	0	98.15	**45**	9	YES
A0A067NAE1_PLEOS	Carbohydrate-binding module family 13 protein	*Pleurotus ostreatus*	0	97.85	**42**	16	YES
A0A067NZH6_PLEOS	Glycoside hydrolase family 105 protein	*Pleurotus ostreatus*	0	94.19	**39**	6	NO
A0A067NZB6_PLEOS	Glycoside hydrolase family 17 protein	*Pleurotus ostreatus*	0	96.76	**31**	0	NO
A0A067NQ10_PLEOS	Alpha-galactosidase	*Pleurotus ostreatus*	0	89.84	**31**	5	YES
A0A067P1X3_PLEOS	Glycoside hydrolase family 16 protein	*Pleurotus ostreatus*	6E-174	96.36	**29**	5	YES
A0A067NLD3_PLEOS	Beta-xylanase	*Pleurotus ostreatus*	0	91.43	**28**	0	YES
A0A067P022_PLEOS	Glycoside hydrolase family 61 protein	*Pleurotus ostreatus*	3E-153	95.78	**28**	6	YES
A0A067NT33_PLEOS	Carbohydrate esterase family 12 protein	*Pleurotus ostreatus*	2E-170	97.64	**25**	1	YES
A0A067P7X8_PLEOS	Glycoside hydrolase family 105 protein	*Pleurotus ostreatus*	0	95.79	**24**	4	YES
V2XER0_MONRO	Alpha beta hydrolase fold family	*Moniliophthora roreri*	7E-155	52.53	**24**	2	NO
V2YA34_MONRO	Arabinofuranosidase	*Moniliophthora roreri*	7E-154	81.85	**20**	3	NO
A0A067NUA1_PLEOS	Glycoside hydrolase family 3 protein	*Pleurotus ostreatus*	0	94.59	**18**	2	NO
A0A067NJP3_PLEOS	Glycoside hydrolase family 28 protein	*Pleurotus ostreatus*	0	96.92	**16**	1	YES
A0A067NTX6_PLEOS	Alpha-galactosidase	*Pleurotus ostreatus*	0	87.31	**14**	2	YES
A0A067PBN9_PLEOS	Glycoside hydrolase family 5 protein	*Pleurotus ostreatus*	0	98.76	**13**	3	YES
A0A0D6A8W8_PLEER	Glucanase	*Pleurotus eryngii*	0	96.29	**13**	4	YES
G3JQR4_CORMM	Glycoside hydrolase, family 25	*Cordyceps militaris*	6E-43	52.78	**13**	1	YES

A0A067P815_PLEOS	Glycoside hydrolase family 61 protein	*Pleurotus ostreatus*	4E-174	96.79	**13**	2	YES
A0A067NUL1_PLEOS	alpha-1,2-Mannosidase	*Pleurotus ostreatus*	0	87.94	**12**	1	YES
A0A067NXU0_PLEOS	Carbohydrate esterase family 4 protein	*Pleurotus ostreatus*	0	96.06	**12**	3	YES
A0A067P1W9_PLEOS	Glycoside hydrolase family 16 protein	*Pleurotus ostreatus*	0	98.77	**12**	8	NO
A0A067P251_PLEOS	Glycoside hydrolase family 3 protein	*Pleurotus ostreatus*	0	95.88	**12**	4	NO
A0A067N637_PLEOS	Glycoside hydrolase family 12 protein	*Pleurotus ostreatus*	4E-171	97.32	**12**	2	YES
A0A067P260_PLEOS	Glycoside hydrolase family 18 protein	*Pleurotus ostreatus*	0	96.61	**10**	1	YES
A0A067P3G0_PLEOS	Glycoside hydrolase family 43 protein	*Pleurotus ostreatus*	0	97.33	**10**	2	YES
A0A067NYF1_PLEOS	Glycoside hydrolase family 16 protein	*Pleurotus ostreatus*	0	92.86	**9**	2	YES
A0A067NUN5_PLEOS	Polysaccharide lyase family 8 protein	*Pleurotus ostreatus*	0	96.44	**9**	1	YES
A0A067N976_PLEOS	Glycoside hydrolase family 18 protein	*Pleurotus ostreatus*	0	95	**8**	4	YES
B0D2X1_LACBS	Cerato-platanin-related secreted protein	*Laccaria bicolor*	2E-45	55.47	**8**	4	YES
A0A067N715_PLEOS	Glycoside hydrolase family 28	*Pleurotus ostreatus*	0	93.01	**7**	3	YES
V2XUY0_MONRO	Glycoside hydrolase family 16 protein	*Moniliophthora roreri*	2E-117	69.41	**7**	3	YES
A0A067NFB3_PLEOS	Beta-galactosidase	*Pleurotus ostreatus*	0	95.38	**7**	4	NO
A0A067P149_PLEOS	Glycoside hydrolase family 31	*Pleurotus ostreatus*	0	95.81	**7**	3	YES
A0A067NPC3_PLEOS	Beta-hexosaminidase	*Pleurotus ostreatus*	0	93.49	**7**	4	YES
A0A067NXA3_PLEOS	Glycoside hydrolase family 28 protein	*Pleurotus ostreatus*	0	82.72	**7**	1	YES
A0A067NYG5_PLEOS	Polysaccharide lyase family 1 protein	*Pleurotus ostreatus*	1E-178	90.38	**7**	1	YES
A0A0D2KN72_9AGAR	Carbohydrate-binding module family 50 protein	*Hypholoma sublateritium*	1E-27	49.56	**6**	0	YES
A0A067NIV2_PLEOS	Glycoside hydrolase family 61 protein	*Pleurotus ostreatus*	5E-116	81.07	**6**	4	YES
A0A067PDP4_9HOMO	Carbohydrate-binding module 1 protein	*Jaapia argillacea*	0	64.91	**6**	1	NO
A0A067P0F8_PLEOS	Glycoside hydrolase family 16 protein	*Pleurotus ostreatus*	0	97.12	**6**	1	YES
A0A067N6T7_PLEOS	Glycoside hydrolase family 3 protein	*Pleurotus ostreatus*	0	94.07	**5**	1	YES
A0A067NXA3_PLEOS	Glycoside hydrolase family 28 protein	*Pleurotus ostreatus*	0	82.72	**5**	2	YES
A0A067NRR9_PLEOS	Polysaccharide lyase family 8 protein	*Pleurotus ostreatus*	0	95.98	**5**	1	YES
A0A067P3Z6_PLEOS	Glycoside hydrolase family 5 protein	*Pleurotus ostreatus*	0	98.48	**5**	1	NO
M5A7J8_GRIFR	Cerato-platanin-like protein 1	*Grifola frondosa*	3E-55	62.67	**5**	1	YES
A0A067NI47_PLEOS	Glycoside hydrolase family 30 protein	*Pleurotus ostreatus*	0	97.18	**4**	0	YES
A0A067P6M4_PLEOS	Carbohydrate-binding module family 13 protein	*Pleurotus ostreatus*	4E-101	92.26	**4**	2	YES
A0A067NX11_PLEOS	Glycoside hydrolase family 92 protein	*Pleurotus ostreatus*	0	93.38	**4**	1	NO
A0A067NUF0_PLEOS	Carbohydrate-binding module family 13 protein	*Pleurotus ostreatus*	2E-104	96.77	**3**	0	YES
A0A067PDE2_PLEOS	Glycoside hydrolase family 55 protein	*Pleurotus ostreatus*	0	97.2	**3**	0	YES
S7S1G5_GLOTA	Glycoside hydrolase	*Gloeophyllum trabeum*	8E-114	48.82	**3**		YES
A0A067NUM1_PLEOS	Glycoside hydrolase family 5 protein	*Pleurotus ostreatus*	0	91.09	**3**	0	YES
G3JQR4_CORMM	Glycoside hydrolase, family 25	*Cordyceps militaris*	6E-43	52.78	**3**	0	NO
A0A067P0T8_PLEOS	Glycoside hydrolase family 88 protein	*Pleurotus ostreatus*	0	93.4	**3**		NO
A0A067NB35_PLEOS	Beta-galactosidase	*Pleurotus ostreatus*	0	90.66	**3**	1	NO
A0A067N6L2_PLEOS	Glycoside hydrolase family 78 protein	*Pleurotus ostreatus*	0	94.12	**3**	1	YES
V2XVB2_MONRO	Glycoside hydrolase family 18 protein	*Moniliophthora roreri*	1E-163	67.47	**3**	1	YES
A0A067NB35_PLEOS	Beta-galactosidase	*Pleurotus ostreatus*	0	90.66	**2**	0	YES
A0A067NHA4_PLEOS	Glycoside hydrolase family 61 protein	*Pleurotus ostreatus*	0	89.46	**2**	0	YES
B0CU10_LACBS	MFS monosaccharide transporter	*Laccaria bicolor*	0	78.8	**2**	0	NO
A0A067NQW1_PLEOS	Trehalase	*Pleurotus ostreatus*	0	95.4	**2**	0	YES
A0A067P685_PLEOS	Arabinogalactan endo-beta-1,4-galactanase	*Pleurotus ostreatus*	0	93.59	**2**	1	YES
A0A067NLV1_PLEOS	Glycoside hydrolase family 79 protein	*Pleurotus ostreatus*	0	96.75	**2**	1	YES
A0A067NL40_PLEOS	Carbohydrate-binding module family 13 protein	*Pleurotus ostreatus*	0	97.31	**2**	1	YES
A0A067P3L9_PLEOS	Carbohydrate esterase family 4 protein	*Pleurotus ostreatus*	0	96.9	**2**	0	YES
A0A0C2XGR8_AMAMU	Glycoside hydrolase family 125 protein	*Amanita muscaria*	0	77.38	**2**	1	NO

(C) PROTEINASES							
Best BLAST non-hypothetical			**E-value**	**Identity (%)**	**Spectral mass counts**		**Signal peptide**
Access number	**Protein description**	**Fungi**			**Average**	**Error**	
A6P7M6_CHLMY	Peptidyl-Lys metalloendopeptidase	*Chlorophyllum molybdites*	2E-149	61.32	**421**	16	YES
V2X6J0_MONRO	Tripeptidyl peptidase a	*Moniliophthora roreri*	0	60.54	**350**	22	YES
Q6ZYK6_PLEOS	Subtilisin-like protease	*Pleurotus ostreatus*	0	97.31	**183**	21	YES
A0A097IYG6_PLEER	Serine proteinase	*Ashbya gossypii*	2E-178	67.52	**119**	3	YES
K9HY03_AGABB	Carboxypeptidase	*Agaricus bisporus var. bisporus*	0	75	**92**	4	YES
A0A067NYE7_PLEOS	Peptide hydrolase	*Pleurotus ostreatus*	0	96.65	**85**	8	YES
V2XDI6_MONRO	Aspartic peptidase a1	*Moniliophthora roreri*	3E-157	57.27	**51**	7	YES
A0A0D7BN91_9HOMO	Extracellular elastinolytic metallo proteinase	*Rhizoctonia solani*	0	65.85	**48**	12	NO
A0A067N455_PLEOS	Peptide hydrolase	*Pleurotus ostreatus*	0	88.81	**47**	1	NO
A0A097IYG6_PLEER	Serine proteinase	*Pleurotus eryngii*	2E-178	67.52	**31**	4	YES
U6A6W7_PLEOS	Aspartic protease	*Pleurotus ostreatus*	0	98.01	**31**	8	YES
X8IWS6_9HOMO	Peptidase family s41 domain protein, putative	*Rhizoctonia solani*	4E-163	41.69	**28**	1	YES
Q8TGE4_COPCI	Leucine aminopeptidase	*Coprinopsis cinerea*	0	72.95	**27**	6	NO
V2XQK0_MONRO	Tripeptidyl peptidase	*Moniliophthora roreri*	0	69.04	**26**	7	YES
S7QH46_GLOTA	Zn-dependent exopeptidase	*Gloeophyllum trabeum*	0	58.73	**24**	8	NO
gi|597911709|ref|XP_007303153.1|	Zn-dependent exopeptidase	*Stereum hirsutum*	0	61.62	**23**	0	NO
gi|597972679|ref|XP_007361264.1|	Creatinase/aminopeptidase [LYAD-421 SS1]	*Dichomitus squalens*	5E-144	51.47	**18**	1	NO
W4JMJ9_9HOMO	Serine protease S8	*Heterobasidion irregulare*	0	64.26	**18**	1	YES
A0A067N859_PLEOS	Peptide hydrolase	*Pleurotus ostreatus*	0	89.87	**17**	4	YES
B0DCT4_LACBS	Aspartic peptidase A1	*Coprinopsis cinerea*	3E-138	53.37	**14**	1	YES
S7RKM8_GLOTA	Acid protease	*Laccaria bicolor*	0	47.68	**14**	2	NO
W4KN38_9HOMO	Aspartic peptidase	*Heterobasidion irregulare*	0	70.77	**10**	3	YES
A0A067NV51_PLEOS	Dipeptidase	*Pleurotus ostreatus*	0	95.74	**7**	1	NO
gi|636607343|ref|XP_008034806.1|	peptidase S28	*Trametes versicolor*	0	68.33	**7**	1	YES
A0A067N7S5_PLEOS	Peptide hydrolase	*Pleurotus ostreatus*	0	93.12	**6**	0	NO
X8IVN7_9HOMO	IgA peptidase M64	*Rhizoctonia solani*	8E-150	49.03	**6**	1	YES
A8NGX3_COPC7	Leucyl aminopeptidase	*Coprinopsis cinerea*	0	64.71	**6**	1	NO
S7S0P1_GLOTA	Peptidase M18, aminopeptidase	*Gloeophyllum trabeum*	0	78.94	**5**	3	NO
A0A067NXD4_PLEOS	Peptide hydrolase	*Pleurotus ostreatus*	0	95.31	**4**	1	YES
A0A067NID9_PLEOS	Peptide hydrolase	*Pleurotus ostreatus*	0	93.9	**4**	4	YES
V2XZJ8_MONRO	Zinc metalloprotease	*Moniliophthora roreri*	0	69.06	**4**	1	NO
W4JQ52_9HOMO	Metallo peptidase M36	*Heterobasidion irregulare*	0	69.98	**3**	1	YES
S8EK55_FOMPI	Proline iminopeptidase	*Fomitopsis pinicola*	0	82.69	**3**	1	NO
B0D4S6_LACBS	Glutamate carboxypeptidase	*Laccaria bicolor*	0	80.92	**2**	1	NO
A0A077K7X8_PLEER	Serine aminopeptidase	*Pleurotus eryngii*	0	80.34	**2**	1	NO

(D) ESTERASES							
Best BLAST non-hypothetical			**E-value**	**Identity (%)**	**Spectral mass counts**		**Signal peptide**
Access number	**Protein description**	**Fungi**			**Average**	**Error**	
A0A067NTY7_PLEOS	Carbohydrate esterase family 4 protein	*Pleurotus ostreatus*	0	97.37	**151**	10	YES
A0A067NAF9_PLEOS	Carboxylic ester hydrolase	*Pleurotus ostreatus*	0	91.54	**84**	11	YES
A0A067NUV8_PLEOS	Pectinesterase	*Pleurotus ostreatus*	0	97.01	**80**	5	YES
A0A067NJF8_PLEOS	Carbohydrate esterase family 4 protein	*Pleurotus ostreatus*	2E-159	91.25	**75**	23	YES
V2YSM2_MONRO	Carbohydrate esterase family 12 protein	*Moniliophthora roreri*	2E-119	67.35	**68**	11	YES
A0A067PBW7_PLEOS	Carboxylic ester hydrolase	*Pleurotus ostreatus*	0	97.14	**54**	4	YES
V6BP73_PLEER	Carboxylic ester hydrolase	*Pleurotus eryngii*	0	99.64	**38**	4	YES
A0A067NPE5_PLEOS	Carbohydrate esterase family 8	*Pleurotus ostreatus*	0	94.12	**37**	0	YES
W4KLA6_9HOMO	Carbohydrate esterase family 4 protein	*Heterobasidion irregulare*	0	75.49	**29**	10	YES
A0A067N5U7_PLEOS	Carbohydrate esterase family 1 protein	*Pleurotus ostreatus*	0	97.56	**28**	4	YES
A0A067NXE9_PLEOS	Carboxylic ester hydrolase	*Pleurotus ostreatus*	0	98.89	**21**	9	YES
A0A067NLL5_PLEOS	Carbohydrate esterase family 4 protein	*Pleurotus ostreatus*	0	96.05	**18**	4	YES
S7RRX7_GLOTA	Carbohydrate esterase family 9 protein	*Gloeophyllum trabeum*	0	62.42	**17**	3	NO
A0A0F7VK25_9AGAR	GDSL like lipase	*Pleurotus sapidus*	0	95.27	**12**	3	YES
gi|599118120|ref|XP_007386740.1|	Lipase	*Punctularia strigosozonata*	2E-137	63.12	**12**	1	YES
A0A067NF84_PLEOS	Carbohydrate esterase family 4 protein	*Pleurotus ostreatus*	0	97.64	**12**	1	YES
V2YES2_MONRO	Carbohydrate esterase family 16 protein	*Moniliophthora roreri*	3E-136	56.95	**10**	8	YES
A0A067N8C4_PLEOS	Carbohydrate esterase family 4 protein	*Pleurotus ostreatus*	2E-176	97.96	**7**	4	YES
A0A067NL12_PLEOS	Carbohydrate esterase family 4 protein	*Pleurotus ostreatus*	0	96.77	**6**	1	YES
B0D886_LACBS	Carbohydrate esterase family 9 protein	*Laccaria bicolor*	0	65.41	**4**	0	NO
A0A067NGD7_PLEOS	Carbohydrate esterase family 4 protein	*Pleurotus ostreatus*	0	97.58	**4**	1	YES
gi|597968945|ref|XP_007360303.1|	PLC-like phosphodiesterase	*Dichomitus squalens*	2E-143	66.9	**2**	0	YES
A0A067NLJ6_PLEOS	Carboxylic ester hydrolase	*Pleurotus ostreatus*	0	94.61	**2**	0	YES

(E) OTHER FUNCTION							
Best BLAST non-hypothetical			**E-value**	**Identity (%)**	**Spectral mass counts**		**Signal peptide**
Access number	**Protein description**	**Fungi**			**Average**	**Error**	
R8BRC1_TOGMI	Putative virulence plasmid b protein	*Togninia minima*	2E-50	23.76	**229**	6	NO
V2WWH5_MONRO	Serine-threonine rich	*Moniliophthora roreri*	2E-21	38.1	**185**	40	YES
V2X6R9_MONRO	Oxalate decarboxylase	*Moniliophthora roreri*	0	74.19	**159**	11	YES
gi|636610047|ref|XP_008036158.1|	Immunomodulatory protein	*Trametes versicolor*	2E-49	65.38	**130**	20	YES
V2XJ06_MONRO	Membrane autotransporter barrel domain protein	*Moniliophthora roreri*	0	62.71	**89**	8	YES
X8J981_9HOMO	Transmembrane protein, putative	*Rhizoctonia solani*	2E-28	36.96	**85**	8	YES
R9AHX0_WALI9	Coiled-coil domain-containing protein	*Wallemia ichthyophaga*	4E-88	64.52	**74**	10	YES
V2YLX4_MONRO	Extracellular dioxygenase	*Moniliophthora roreri*	2E-94	53.44	**72**	8	YES
Q75VR2_PLEER	Ribonuclease T2	*Pleurotus eryngii*	0	91.06	**61**	4	YES
M2PP67_CERS8	CsMn38	*Ceriporiopsis subvermispora*	1E-32	52.67	**59**	13	YES
A0A086T8T8_ACRCH	Mediator of RNA polymerase II transcription subunit-like protein	*Acremonium chrysogenum*	2.3	31.33	**51**	1	NO
A0A0A1UUM1_9HYPO	Ketosteroid isomerase-like protein	*Metarhizium robertsii*	0.0005	28.67	**51**	6	YES
I6UR56_ENCHA	Cyclin-dependent protein	*Encephalitozoon hellem*	0.004	28.07	**48**	18	YES
V2YLU2_MONRO	Nhl repeat-containing protein	*Moniliophthora roreri*	1E-154	55.33	**46**	3	YES

gi|636607513|ref|XP_008034891.1|	Galactose mutarotase-like protein	*Trametes versicolor*	0	71.15	**44**	0	YES
A0A067NZB1_PLEOS	S-adenosylmethionine synthase	*Pleurotus ostreatus*	0	99.48	**40**	4	NO
Q753M7_ASHGO	AFR285Cp	*Ashbya gossypii*	3E-50	100	**40**	2	NO
A0A0D7BTI4_9HOMO	Class I glutamine amidotransferase-like protein	*Rhizoctonia solani*	2E-81	57.01	**39**	2	NO
M5BXC7_THACB	Pathogenesis-related protein 5	*Thanatephorus cucumeris*	8E-143	78.04	**38**	2	YES
B1Q4S7_PLEOS	Ribonuclease T1	*Pleurotus ostreatus*	1E-81	95.24	**35**	3	YES
Q9P356_LENED	Nuclease Le1	*Lentinula edodes*	5E-105	62.18	**35**	1	NO
V2WHJ4_MONRO	Chitin synthase	*Moniliophthora roreri*	4E-11	34.93	**35**	0	NO
V2XER0_MONRO	Alpha beta hydrolase fold family	*Moniliophthora roreri*	7E-155	52.53	**35**	2	NO
G9MD63_PLEOS	Glyceraldehyde-3-phosphate dehydrogenase	*Pleurotus ostreatus*	0	100	**32**	4	NO
A0A074S4Z0_9HOMO	Putative Ran-binding protein	*Rhizoctonia solani*	2E-94	66.05	**31**	4	YES
G4THH4_PIRID	Related to TY3B-TY3B protein	*Piriformospora indica*	0.73	27.27	**28**	6	NO
A0A067P1S4_PLEOS	Aspartate aminotransferase	*Pleurotus ostreatus*	0	97.8	**28**	1	NO
V2XHH7_MONRO	Fad binding domain-containing protein	*Moniliophthora roreri*	5E-150	45.68	**27**	4	YES
A0A067NPM1_PLEOS	Superoxide dismutase	*Pleurotus ostreatus*	1E-118	89.23	**27**	8	NO
V2XBH5_MONRO	Formate dehydrogenase	*Moniliophthora roreri*	0	87.64	**26**	1	NO
A0A0A8IBD8_PLEOS	Lipoxygenase	*Pleurotus ostreatus*	0	97.51	**26**	4	NO
A0A067NEK4_PLEOS	Peptidyl-prolyl cis-trans isomerase	*Pleurotus ostreatus*	3E-110	96.91	**26**	5	NO
gi|595777092|ref|XP_007267089.1|	Alpha/beta-hydrolase	*Fomitiporia mediterranea*	3E-69	44.33	**24**	4	YES
gi|597901894|ref|XP_007298246.1|	Dienelactone hydrolase	*Stereum hirsutum*	2E-168	82.18	**23**	0	NO
gi|628835621|ref|XP_007768114.1|	Alpha beta-hydrolase	*Coniophora puteana*	1E-145	59.52	**23**	4	YES
E2LF87_MONPE	Enolase	*Moniliophthora perniciosa*	0	95.58	**21**	6	NO
A0A067NCD3_PLEOS	Transaldolase	*Pleurotus ostreatus*	0	98.77	**20**	3	NO
gi|597911309|ref|XP_007302953.1|	Cobalamin-independent methionine synthase	*Stereum hirsutum*	0	85.36	**20**	3	NO
V2WXW2_MONRO	Major royal jelly protein	*Moniliophthora roreri*	0	68.3	**20**	7	NO
X8JFA9_9HOMO	Cytochrome b2 (L-lactate ferricytochrome C oxidoreductase)	*Rhizoctonia solani*	2E-121	55.98	**20**	5	YES
V2X4P6_MONRO	Acetyl-hydrolase	*Moniliophthora roreri*	0	82.2	**20**	2	NO
A0A0D7BIU0_9HOMO	Cupredoxin	*Rhizoctonia solani*	2E-98	51.98	**20**	1	YES
S7PXC3_GLOTA	Malate dehydrogenase	*Gloeophyllum trabeum*	5E-71	48.73	**19**	1	YES
X8JM78_9HOMO	GEgh 16 protein, putative	*Rhizoctonia solani*	7E-83	70.97	**17**	1	YES
A0A067NID3_PLEOS	tRNA pseudouridine synthase	*Pleurotus ostreatus*	0	84.28	**17**	1	NO
gi|599119355|ref|XP_007387147.1|	NAD(P)-binding protein	*Punctularia strigosozonata*	1E-104	62.99	**15**	1	NO
V2X1Q4_MONRO	Fumarylacetoacetate hydrolase domain-containing protein 2a	*Moniliophthora roreri*	7E-137	63.37	**15**	6	YES
A8NBU8_COPC7	Carbonic anhydrase	*Coprinopsis cinerea*	3E-50	53.94	**14**	3	NO
S7PXC3_GLOTA	Malate dehydrogenase	*Gloeophyllum trabeum*	5E-71	48.73	**13**	3	YES
V2XER0_MONRO	Alpha beta hydrolase fold family	*Moniliophthora roreri*	7E-155	52.53	**13**	6	YES
Q9C1M8_PLESA	Catalase	*Pleurotus sajor-caju*	0	97.35	**13**	2	NO
gi|595777736|ref|XP_007267411.1|	Amidase signature enzyme	*Fomitiporia mediterranea*	0	77.52	**13**	8	NO
A0A0D7BR14_9HOMO	Aldehyde dehydrogenase	*Cylindrobasidium torrendii*	0	73.19	**11**	1	NO
A0A0C6DUW9_GRIFR	Gf.ODC1 protein	*Polyporus frondosus*	0	72.27	**11**	1	YES
A0A086TGA7_ACRCH	Serine/threonine-protein kinase-like protein	*Acremonium chrysogenum*	0.007	31.31	**11**	4	YES
A0A074S9X6_9HOMO	Putative six-hairpin glycosidase-like protein	*Rhizoctonia solani*	0	54.79	**11**	4	YES
B0DJI3_LACBS	Ectomycorrhiza-regulated small secreted protein	*Laccaria bicolor*	0.37	22.56	**10**	5	YES
M2PP67_CERS8	CsMn38	*Ceriporiopsis subvermispora*	1E-32	52.67	**10**	6	YES
G4THH4_PIRID	Related to TY3B-TY3B protein	*Piriformospora indica*	0.73	27.27	**10**	1	NO
V2WRU0_MONRO	Putative actin filament organization protein App1-like	*Moniliophthora roreri*	1E-115	51.08	**9**	0	YES

B0E0N3_LACBS	NADP-dependent mannitol dehydrogenase MtDH	*Laccaria bicolor*	7E-151	78.24	**9**	4	NO
A0A0C3FTH1_9HOMO	Glucooligosaccharide oxidase	*Rhizoctonia solani*	6E-158	54.77	**9**	1	YES
V2WRN7_MONRO	Macrofage activating glycoprotein	*Moniliophthora roreri*	7E-148	59.83	**9**	1	YES
A0A067NZL3_PLEOS	Transaldolase	*Pleurotus ostreatus*	0	98.77	**8**	1	NO
V2XDY3_MONRO	D-lactonohydrolase-like protein	*Moniliophthora roreri*	0	74.39	**8**	3	NO
A0A074RKL3_9HOMO	Ferritin-like protein	*Rhizoctonia solani*	1E-18	36.9	**8**	3	NO
A0A067NUP7_PLEOS	Aspartate aminotransferase	*Pleurotus ostreatus*	0	99.06	**8**	1	NO
L8WU55_THACA	SKG6 domain-containing protein	*Thanatephorus cucumeris*	7E-47	37.74	**8**	2	YES
A0A067NKD5_PLEOS	Peptidyl-prolyl cis-trans isomerase	*Pleurotus ostreatus*	8E-87	93.94	**8**	1	NO
A0A0A8L9E4_9SACH	Coatomer subunit alpha	*Kluyveromyces dobzhanskii*	5.7	31.08	**8**	1	NO
A0A074RTR7_9HOMO	Protein transporter Sec23	*Rhizoctonia solani*	1E-51	40.43	**8**	1	NO
V2XK68_MONRO	Dj-1 family protein	*Moniliophthora roreri*	2E-97	65.12	**8**	1	YES
X8IX14_9HOMO	Ferritin-like protein	*Rhizoctonia solani*	0.000006	32.09	**8**	2	NO
V2YID8_MONRO	Vacuolar protein	*Moniliophthora roreri*	0	65.38	**7**	3	YES
A0A067NH04_PLEOS	Profilin	*Pleurotus ostreatus*	2E-74	90.48	**7**	1	NO
B6HJZ8_PENCW	Pc21g02480 protein	*Penicillium chrysogenum*	8E-12	35.9	**7**	1	YES
D2JY76_PLEOS	Superoxide dismutase	*Pleurotus ostreatus*	8E-118	97.24	**7**	5	NO
M5G747_DACSP	DUTP diphosphatase	*Dacryopinax sp.*	2E-86	91.97	**7**	4	NO
V2WRN7_MONRO	Macrofage activating glycoprotein	*Moniliophthora roreri*	7E-148	59.83	**7**	1	YES
A0A074S4Z0_9HOMO	Putative Ran-binding protein	*Rhizoctonia solani*	2E-94	66.05	**7**	2	YES
G7XH64_ASPKW	Similar to An15g00620	*Aspergillus kawachii*	5E-09	31.43	**7**	2	NO
A0A0B4GK80_9HYPO	FAD binding domain-containing protein	*Metarhizium brunneum*	2.6	30.28	**7**	1	NO
S7RVM0_GLOTA	Phytase	*Gloeophyllum trabeum*	0	62.78	**7**	1	NO
A0A0D1E1U3_USTMA	Chromosome 5, whole genome shotgun sequence	*Ustilago maydis*	1E-10	28.57	**6**	4	YES
gi|597971127|ref|XP_007360861.1|	Cofactor-independent phosphoglycerate mutase	*Dichomitus squalens*	0	80.46	**6**	3	NO
V2Y6M8_MONRO	Ornithine aminotransferase	*Moniliophthora roreri*	0	80.09	**6**	1	NO
A8NV50_COPC7	WSC domain-containing protein	*Coprinopsis cinerea (*	8E-162	60.7	**6**	1	YES
V2WGW3_MONRO	Aldolase citrate lyase family protein	*Moniliophthora roreri*	6E-117	64.55	**6**	2	NO
gi|599112879|ref|XP_007385021.1|	Eliciting plant response-like protein	*Punctularia strigosozonata*	4E-40	60.19	**6**	1	NO
V2XHB5_MONRO	Hesp-379-like protein	*Moniliophthora roreri*	5E-41	45.24	**6**	2	YES
gi|595786154|ref|XP_007271620.1|	PEBP-like protein	*Fomitiporia mediterranea*	9E-67	56.44	**6**	4	YES
V2XD50_MONRO	Short-chain dehydrogenase reductase sdr	*Moniliophthora roreri*	2E-120	68.38	**6**	1	NO
V2W6S8_MONRO	Epoxide hydrolase	*Moniliophthora roreri*	4E-116	50.61	**6**	2	NO
H1AFL5_PLEOS	Glyceraldehyde-3-phosphate dehydrogenase	*Pleurotus ostreatus*	0	98.98	**5**	3	NO
V2YGF9_MONRO	Chitin binding	*Moniliophthora roreri*	2E-77	63.01	**5**	0	YES
A0A0D7BAF1_9HOMO	Inorganic diphosphatase	*Cylindrobasidium torrendii*	0	88.18	**5**	0	NO
L8WD12_THACA	GPI-anchored domain-containing protein	*Rhizoctonia solani*	2E-27	46.4	**5**	1	YES
A0A0B2X373_9HYPO	Extracellular serine-rich protein	*Metarhizium album*	2E-20	44.6	**5**	0	YES
gi|628838035|ref|XP_007769308.1|	Heat shock protein	*Coniophora puteana*	0	89.32	**5**	2	NO
V2X3A6_MONRO	Serine-threonine protein phosphatase	*Moniliophthora roreri*	6E-178	72.98	**5**	1	YES
gi|636620133|ref|XP_008041201.1|	D-lactonohydrolase-like protein	*Trametes versicolor*	2E-142	54.93	**5**	1	YES
A0A0A1ULS1_9HOMO	Ricin-type beta-trefoil lectin domain protein	*Rhizoctonia solani*	3.1	27.68	**5**	1	NO
B0CU00_LACBS	Phosphoglucomutase	*Laccaria bicolor*	0	84.42	**5**	1	NO
S7Q8D4_GLOTA	Sure-like protein	*Gloeophyllum trabeum*	5E-116	59.79	**5**	4	YES
A0A0H2STW2_9HOMO	Cupredoxin	*Schizopora paradoxa*	2E-95	43.38	**5**	1	YES
gi|597907694|ref|XP_007301146.1|	Heat shock protein 70	*Stereum hirsutum*	0	94.27	**4**	3	NO
A0A067N5Y3_PLEOS	Dihydrolipoyl dehydrogenase	*Pleurotus ostreatus*	0	98.23	**4**	1	NO
V2XB56_MONRO	Neutral ceramidase	*Moniliophthora roreri*	0	70.99	**4**	0	YES
V2X4R1_MONRO	Stomatin family protein	*Moniliophthora roreri*	0	80.74	**4**	1	NO

gi|595777092|ref|XP_007267089.1|	Alpha/beta-hydrolase	*Fomitiporia mediterranea*	3E-69	44.33	**4**	3	YES
gi|628829085|ref|XP_007764846.1|	FAS1 domain-containing protein	*Coniophora puteana*	5E-81	35.28	**4**	0	YES
V2YHR5_MONRO	Abhydrolase domain-containing protein 12	*Moniliophthora roreri*	5E-129	49.23	**4**	1	NO
A0A0D7AGU2_9AGAR	Arginase/deacetylase	*Fistulina hepatica*	0	78.12	**4**	0	YES
A0A099P3U9_PICKU	Serine/threonine-protein kinase	*Pichia kudriavzevii*	2.8	28.3	**4**	3	NO
R7S5S7_PUNST	GroES-like protein	*Punctularia strigosozonata*	0.46	31.36	**4**		NO
B6GW49_PENCW	Pc06g01100 protein	*Penicillium chrysogenum*	2E-22	34.8	**4**		NO
V2XJA5_MONRO	Cellular morphogenesis protein	*Moniliophthora roreri*	0	57.77	**4**	1	YES
V2XIT2_MONRO	Glutamyl-trna amidotransferase subunit a	*Moniliophthora roreri*	0	72.69	**4**		NO
V2WVC1_MONRO	Phosphatidylserine decarboxylase	*Moniliophthora roreri*	0	72.85	**4**	2	NO
A0A067NS53_PLEOS	Pyruvate carboxylase	*Pleurotus ostreatus*	0	99	**4**	2	NO
A0A067NYN3_PLEOS	6,7-dimethyl-8-ribityllumazine synthase	*Pleurotus ostreatus*	2E-151	98.58	**4**	2	NO
X8JFM1_9HOMO	Transmembrane protein, putative	*Rhizoctonia solani*	5E-42	30.1	**4**	1	NO
V2XHI8_MONRO	Phospholipase C/P1 nuclease	*Moniliophthora roreri*	5E-149	54	**4**	1	YES
V2X5R0_MONRO	Immunomodulatory protein	*Pleurotus ostreatus*	8E-09	26.78	**4**	1	YES
A0A067N4P4_PLEOS	OPT superfamily	*Pleurotus ostreatus*	0	97.58	**4**	1	NO
V2XPL7_MONRO	Fumarylacetoacetate hydrolase	*Moniliophthora roreri*	5E-165	74.34	**4**	1	NO
A0A067N7N9_PLEOS	Fet3 ferroxidase	*Pleurotus ostreatus*	0	98.73	**4**	1	YES
V2YRZ7_MONRO	Gpi-anchored small secreted protein	*Moniliophthora roreri*	6E-26	41.13	**4**	1	YES
V2XAL1_MONRO	Guanine nucleotide binding protein beta subunit 2	*Moniliophthora roreri*	0	96.29	**3**	0	NO
V2XDS5_MONRO	Fumarate reductase	*Moniliophthora roreri*	0	84.3	**3**		NO
A0A0D7B1T3_9HOMO	1-Cys peroxiredoxin isozyme	*Cylindrobasidium torrendii*	8E-93	78.36	**3**		NO
V2X374_MONRO	Sub60s ribosomal protein	*Moniliophthora roreri*	7E-117	90.32	**3**		NO
S7QCY4_GLOTA	Sm-like ribonucleo protein	*Gloeophyllum trabeum*	1E-79	95.31	**3**		NO
A0A067NV87_PLEOS	Glucose-6-phosphate isomerase	*Pleurotus ostreatus*	0	99.09	**3**		NO
A0A067TDZ6_9AGAR	3,4-dihydroxy-2-butanone 4-phosphate synthase	*Galerina marginata*	1E-121	66.27	**3**		NO
V2XER0_MONRO	Alpha beta hydrolase fold family	*Moniliophthora roreri*	7E-155	52.53	**3**	0	YES
X8IZK9_9HOMO	Allergen protein	*Rhizoctonia solani*	3E-81	72.62	**3**	0	YES
A0A0C3G6Z6_9HOMO	Imidazoleglycerol-phosphate dehydratase	*Piloderma croceum*	8E-135	91.54	**3**	0	NO
W4JRY9_9HOMO	Lep6-lignin expressed protein 6	*Heterobasidion irregulare*	5E-28	27.58	**3**	0	NO
V2WWY6_MONRO	Hydrophobic surface binding protein	*Moniliophthora roreri*	4E-48	52.46	**3**	3	YES
A0A074S8Y2_9HOMO	Putative transmembrane protein	*Rhizoctonia solani*	1E-76	43.57	**3**	3	YES
A0A0H2S0W7_9HOMO	Gamma-glutamyltranspeptidase	*Schizopora paradoxa*	0	69.31	**3**		NO
V2XWZ3_MONRO	Putative aminotransferase	*Moniliophthora roreri*	0	69.04	**3**		NO
E4ZP67_LEPMJ	Similar to stress responsive alpha-beta barrel domain-containing protein	*Leptosphaeria maculans*	0.00009	29.25	**3**	1	NO
gi|597976059|ref|XP_007362138.1|	4-carboxymuconolactone decarboxylase	*Dichomitus squalens*	2E-83	65.97	**3**	0	YES
V2XVV7_MONRO	Er to golgi transport-related protein	*Moniliophthora roreri*	4E-60	39.41	**3**	1	NO
Q96TU2_PLEOS	Cap64 protein	*Pleurotus ostreatus*	0	97.85	**3**		NO
A0A0H2RUN5_9HOMO	Short-chain dehydrogenase	*Schizopora paradoxa*	4E-168	82.69	**3**		NO
V2Y1X1_MONRO	Mitochondrial protein	*Moniliophthora roreri*	8E-108	65.15	**3**	1	NO
gi|636607613|ref|XP_008034941.1|	Ribosomal protein S25 [Trametes versicolor FP-101664 SS1]	*Trametes versicolor*	7E-41	84.31	**3**	1	NO
Q6L660_PLEOS	Ribonuclease T2	*Pleurotus ostreatus*	0	95.42	**3**	2	YES
K9I1K6_AGABB	XCL-like lectin	*Agaricus bisporus var. bisporus*	2E-22	40.56	**3**	1	NO
gi|597903154|ref|XP_007298876.1|	metal-dependent protein hydrolase	*Stereum hirsutum*	1E-179	73.17	**3**	1	NO
A0A0D7AQF0_9AGAR	Flavocytochrome c	*Fistulina hepatica*	0	63.97	**3**	2	NO

A0A0H2R6D9_9HOMO	PEBP-like protein	*Schizopora paradoxa*	3E-79	56.7	**3**	1	YES
V2XRT0_MONRO	Serine-threonine rich	*Moniliophthora roreri*	8E-43	64.41	**3**	1	YES
A0A0D7B8B9_9HOMO	Acetamidase/Formamidase	*Cylindrobasidium torrendii*	0	86.97	**3**	1	NO
S4S6Z0_HEBCY	L-amino acid oxidase	*Hebeloma cylindrosporum*	3E-175	50.46	**3**	1	NO
gi|599094462|ref|XP_007378965.1|	heparinase II/III family protein	*Punctularia strigosozonata*	0	64.8	**3**	2	NO
X8IZK9_9HOMO	Allergen protein	*Rhizoctonia solani*	3E-81	72.62	**3**	1	YES
S7QKA7_GLOTA	Ribosomal protein S4	*Gloeophyllum trabeum*	1E-122	97.81	**2**		NO
A0A067NHP6_PLEOS	40S ribosomal protein S0	*Pleurotus ostreatus*	0	96.96	**2**		NO
A0A0D7A525_9AGAR	Nucleic acid-binding protein	*Fistulina hepatica*	3E-63	60.81	**2**		NO
NNRD_COPC7	ATP-dependent (S)-NAD(P)H-hydrate dehydratase	*Coprinopsis cinerea*	0	72.43	**2**		NO
A0A067NQ58_PLEOS	Proteasome subunit beta type	*Pleurotus ostreatus*	8E-178	99.59	**2**	0	NO
R7S4L7_PUNST	NAD(P)-binding protein	*Punctularia strigosozonata*	2E-108	71.08	**2**		NO
A0A0C2ZFM7_9HOMO	Transcription elongation factor	*Scleroderma citrinum*	0.52	26.39	**2**	0	NO
V2XWI1_MONRO	NAD-P-binding protein	*Moniliophthora roreri*	4E-120	53.17	**2**		NO
S7RD10_GLOTA	Dioxygenase family protein	*Gloeophyllum trabeum*	3E-154	68.21	**2**	0	NO
S7QCY7_GLOTA	Nonaspanin	*Gloeophyllum trabeum*	0	81.86	**2**	0	YES
A0A074RH65_9HOMO	Putative transmembrane protein	*Rhizoctonia solani*	1	25.88	**2**		NO
X8JNF1_9HOMO	Mucoidy inhibitor A, putative	*Rhizoctonia solani*	1E-54	26.93	**2**		NO
T2HUL2_PLEER	Pe.pleurotolysin A	*Pleurotus eryngii*	1E-96	100	**2**		NO
X8JCL8_9HOMO	Retrotransposon gag protein	*Rhizoctonia solani*	0.4	24.21	**2**	1	NO
W4K568_9HOMO	ABC transporter	*Heterobasidion irregulare*	0	63.43	**2**		NO
V2YXX7_MONRO	Prenylated rab acceptor 1	*Moniliophthora roreri*	3E-86	73.78	**2**	0	NO
R7T2T7_DICSQ	Small GTPase-binding protein	*Dichomitus squalens*	1E-134	94.85	**2**	0	NO
V2XST8_MONRO	Fad binding domain protein	*Moniliophthora roreri*	0	55.74	**2**	1	YES
L8WS14_THACA	KapM protein	*Thanatephorus cucumeris*	5E-16	34.07	**2**		YES
R7SSC4_DICSQ	Anthranilate phosphoribosyltransferase	*Dichomitus squalens*	2E-29	59.48	**2**		YES
V2WVC8_MONRO	Aminoacylase 1-like protein 2	*Moniliophthora roreri*	0	59.92	**2**		NO
B6HJZ8_PENCW	Pc21g02480 protein	*Penicillium chrysogenum*	8E-12	35.9	**2**		YES
S7QJ37_GLOTA	Multidrug efflux transporter AcrB transmembrane domain-containing protein	*Gloeophyllum trabeum*	0	71.6	**2**		NO
A8NPZ1_COPC7	YjgH family protein	*Coprinopsis cinerea*	5E-50	67.86	**2**		NO
gi|636608055|ref|XP_008035162.1|	aflatoxin-detoxifizyme	*Trametes versicolor*	0	77.97	**2**		NO
A0A067P0D5_PLEOS	Glycosyltransferase family 2 protein	*Pleurotus ostreatus*	0	96.74	**2**		NO
gi|597912997|ref|XP_007303797.1|	WD40 repeat-like protein	*Stereum hirsutum*	0	61.21	**2**		NO
gi|628827991|ref|XP_007764299.1|	Carbon-nitrogen hydrolase	*Coniophora puteana*	1E-171	72.85	**2**		NO
B0DW71_LACBS	Ectomycorrhiza-regulated small secreted protein	*Laccaria bicolor*	6E-27	43.97	**2**		YES
V2XHI7_MONRO	2-nitro propane dioxygenase	*Moniliophthora roreri*	4E-112	50	**2**		NO
A0A067NUG5_PLEOS	Non-specific serine/threonine protein kinase	*Pleurotus ostreatus*	0	95.03	**2**		NO
A0A066XCF5_COLSU	Putative RhoGEF domain-containing protein	*Colletotrichum sublineola*	0.32	35.09	**2**		NO
V2WUN4_MONRO	TPR-likeprotein	*Moniliophthora roreri*	7E-87	33.52	**2**		NO
A0A067NN37_PLEOS	Plant-expansin-like protein	*Pleurotus ostreatus*	1E-91	99.22	**2**		YES
S9Q159_SCHOY	BRCT domain-containing protein Brc1	*Schizosaccharomyces octosporus*	0.49	29.85	**2**		NO
V2WU96_MONRO	F-box domain protein	*Moniliophthora roreri*	5E-66	31.31	**2**		NO
A0A0B1PAT4_UNCNE	Putative cyclin-like f-box protein	*Uncinula necator*	3E-86	48.6	**2**	1	NO
V2XG03_MONRO	Short chain type	*Moniliophthora roreri*	2E-72	49.79	**2**	1	NO

(F) UNKNOWN FUNCTION							
Best BLAST non-hypothetical			**E-value**	**Identity (%)**	**Spectral mass counts**		**Signal peptide**
Access number	**Protein description**	**Fungi**			**Average**	**Error**	
D8PY21_SCHCM	Expressed protein	*Schizophyllum commune*	2E-11	35	**152**	31	NO
V2X669_MONRO	Secreted protein	*Moniliophthora roreri*	2E-32	45.56	**55**	7	YES
D8Q129_SCHCM	Expressed protein	*Schizophyllum commune*	2E-17	32.81	**52**	6	YES
A0A067NYR7_PLEOS	Evidence of expression at protein level	*Pleurotus ostreatus*	0	95.16	**38**	3	NO
D8PY21_SCHCM	Expressed protein	*Schizophyllum commune*	2E-11	35	**36**	3	YES
D8PXC2_SCHCM	Expressed protein	*Schizophyllum commune*	0.004	24.02	**29**	1	YES
B0CXV6_LACBS	GPI-anchored small secreted protein	*Laccaria bicolor*	1E-38	53.47	**25**	1	YES
A0A074SC17_9HOMO	DUF4243 family protein 123E	*Rhizoctonia solani*	1E-108	42.58	**15**	1	NO
J4UG46_BEAB2	Putative secreted protein	*Beauveria bassiana*	0.000005	26.35	**14**	4	NO
gi|595769286|ref|XP_007263186.1|	DUF427-domain-containing protein [MF3/22]	*Fomitiporia mediterranea*	3E-109	66.12	**12**	0	NO
gi|636618993|ref|XP_008040631.1|	Sure-like protein	*Trametes versicolor*	2E-106	54.9	**9**	1	YES
D8QIL5_SCHCM	Expressed protein	*Schizophyllum commune*	6E-12	33.62	**9**	3	YES
D8Q6X5_SCHCM	Expressed protein	*Schizophyllum commune*	2E-84	77.33	**8**	1	YES
D8Q1J2_SCHCM	Expressed protein	*Schizophyllum commune*	8E-33	36.29	**8**	0	NO
D8QD03_SCHCM	Expressed protein	*Schizophyllum commune*	2E-07	38.24	**6**	0	YES
K9I8U3_AGABB	Secreted protein	*Agaricus bisporus var. bisporus*	5E-92	47.19	**6**	2	YES
J0WWW8_AURDE	DUF427-domain-containing protein	*Auricularia delicata*	3E-43	69.89	**4**	0	NO
V2XTV0_MONRO	Secreted protein	*Moniliophthora roreri*	1E-75	52.28	**3**	0	NO
W6MS03_9ASCO	Genomic scaffold	*Kuraishia capsulata*	0.00006	25.61	**3**	0	YES
X8JBR9_9HOMO	CHCH domain protein	*Rhizoctonia solani*	2E-56	31.12	**3**	0	NO
W6QVQ8_PENRO	Genomic scaffold, ProqFM164S03	*Penicillium roqueforti*	7E-28	42.86	**3**	1	YES
D8Q6X5_SCHCM	Expressed protein	*Schizophyllum commune*	2E-84	77.33	**2**	1	YES
D8PZF9_SCHCM	Expressed protein	*Schizophyllum commune*	4E-54	54.38	**2**	1	NO
D8PNW9_SCHCM	Expressed protein	*Schizophyllum commune*	7E-164	53.75	**2**	1	YES